Molecular Therapy
Methods & Clinical Development
Original Article

Safe and Effective Gene Therapy for Murine Wiskott-Aldrich Syndrome Using an Insulated Lentiviral Vector

Swati Singh,[1] Iram Khan,[1] Socheath Khim,[1] Brenda Seymour,[1] Karen Sommer,[1] Matthew Wielgosz,[2] Zachary Norgaard,[3] Hans-Peter Kiem,[3,4] Jennifer Adair,[3,5] Denny Liggitt,[6] Arthur Nienhuis,[2] and David J. Rawlings[1,7,8]

[1]Center for Immunity and Immunotherapies and Program for Cell and Gene Therapy, Seattle Children's Research Institute, Seattle, WA 98101, USA; [2]Department of Hematology, St. Jude Children's Research Hospital, Memphis, TN 38105, USA; [3]Clinical Research Division, Fred Hutchinson Cancer Research Center, Seattle, WA 98109, USA; [4]Department of Pathology, University of Washington, Seattle, WA 98105, USA; [5]Department of Medical Oncology, University of Washington, Seattle, WA 98105, USA; [6]Department of Comparative Medicine, University of Washington, Seattle, WA 98105, USA; [7]Department of Pediatrics, University of Washington, Seattle, WA 98105, USA; [8]Department of Immunology, University of Washington, Seattle, WA 98105, USA

Wiskott-Aldrich syndrome (WAS) is a life-threatening immunodeficiency caused by mutations within the *WAS* gene. Viral gene therapy to restore WAS protein (WASp) expression in hematopoietic cells of patients with WAS has the potential to improve outcomes relative to the current standard of care, allogeneic bone marrow transplantation. However, the development of viral vectors that are both safe and effective has been problematic. While use of viral transcriptional promoters may increase the risk of insertional mutagenesis, cellular promoters may not achieve WASp expression levels necessary for optimal therapeutic effect. Here we evaluate a self-inactivating (SIN) lentiviral vector combining a chromatin insulator upstream of a viral MND (MPSV LTR, NCR deleted, dl587 PBS) promoter driving WASp expression. Used as a gene therapeutic in *Was*$^{-/-}$ mice, this vector resulted in stable WASp^{+} cells in all hematopoietic lineages and rescue of T and B cell defects with a low number of viral integrations per cell, without evidence of insertional mutagenesis in serial bone marrow transplants. In a gene transfer experiment in non-human primates, the insulated MND promoter (driving GFP expression) demonstrated long-term polyclonal engraftment of GFP^{+} cells. These observations demonstrate that the insulated MND promoter safely and efficiently reconstitutes clinically effective WASp expression and should be considered for future WAS therapy.

INTRODUCTION

Wiskott-Aldrich syndrome (WAS) is an X-linked primary immunodeficiency disease resulting from mutations within the *WAS* gene that result in the loss of WAS protein (WASp) or function. Subjects with WAS suffer from combined immunodeficiency, thrombocytopenia, and eczema and also frequently develop autoimmunity and lymphoid malignancies.[1–4] WASp is a scaffold protein involved in signal transduction pathways that activate the actin cytoskeleton downstream of multiple cell surface receptors, including the B and T cell antigen receptors.[5–7] Although the disease phenotype can be alleviated with hematopoietic stem cell transplantation (HSCT), the success of this therapy is variable, depending on factors such as the patient's age, donor compatibility, conditioning regimen, and the extent of reconstitution. In the absence of a histocompatibility leukocyte antigen (HLA)-matched donor, transplantation with a mismatched donor has a reduced survival rate.[3,8,9] Since the phenotype of WAS deficiency impacts only hematopoietic cells, gene therapy is a possible alternative. In this approach, a WASp expression cassette is stably integrated into the chromatin of autologous hematopoietic stem cells (HSCs) using viral-based gene delivery.

Previous and ongoing clinical trials have demonstrated the efficacy of gene therapy for alleviating the pathologies of WAS.[10–12] Importantly, following development of T cell leukemia due to insertional mutagenesis in γ-retroviral gene therapy trials for both severe combined immunodeficiency (SCID) and WAS,[13–15] much research has focused on strategies for eliminating this risk. The use of self-inactivating (SIN) lentiviruses (LVs) for gene transfer is one critical improvement, combining a safer integration profile (less affinity for insertions near promoters than γ-retroviruses[16–18]) with the ability to select internal promoters that optimize transgene expression and safety.[19] Because of the association between internal promoter strength and transformation potential,[19] internal promoters are selected for their ability to recapitulate endogenous expression levels and regulation, as well as for the lack of transactivation potential both in vitro and in vivo. These considerations are particularly important for treating WAS based on the following findings: sub-endogenous levels of WASp

Received 30 July 2016; accepted 15 November 2016;
http://dx.doi.org/10.1016/j.omtm.2016.11.001.

Correspondence: David J. Rawlings, Center for Immunity and Immunotherapies, Seattle Children's Research Institute, 1900 Ninth Avenue, Seattle, WA 98101, USA.
E-mail: drawling@uw.edu

expression may hinder the reconstitution of murine B cell, T cell, and myeloid subsets and platelets;[20] insufficient WASp expression in B cells compared to T cells can drive acquisition of autoimmunity;[21–23] and patients with WAS are predisposed to malignancies and clonal expansion.[1,3,4] Current clinical trials for WAS utilize a SIN-LV with an internal promoter consisting of the proximal 1.6 kb of the endogenous *WAS* promoter (WS1.6) to drive human WASp (hWASp) expression.[10,12] Patients treated with this SIN-LV showed improvements in immunity to infections, resolved eczema, and protection from bleeding, without evidence of clonal expansion of cells[10,12] or loss of self-tolerance.[24,25] However, clinical improvement required relatively high levels of viral marking and alleviation of the WAS phenotype was incomplete with, most notably, limited or no improvement in platelet counts. In previous mouse gene therapy experiments, we found that the WS1.6 promoter did not effectively rescue WASp expression in all lineages including B cells and resulted in the acquisition of features of humoral autoimmunity.[20] In contrast, an SIN-LV using a synthetic promoter derived from a γ-retrovirus called MND (MPSV LTR, NCR deleted, dl587 PBS)[26] as an internal promoter rescued WASp expression in all affected lineages and reduced the risk of autoimmunity.[20,27,28]

In a clinical gene therapy trial for adrenoleukodystrophy, MND has been used as an internal promoter for LV gene therapy without adverse effects.[29] Although strongly *trans*-activating promoters are associated with an enhanced risk of insertional transactivation, this risk can be diminished by including a chromatin insulator.[28,30,31] Chromatin insulators act as boundary elements preventing interactions between adjacent chromatin domains.[32–34] Candidate insulator constructs can function as "barrier only" elements (acting as barriers to epigenetic chromatin silencing) or "enhancer-blocker only" elements (that prevent promoter transactivation between the domains that they separate), or they can have both activities (as reviewed in Emery et al.[35] and Raab et al.[36]). One of the best characterized insulators, chicken β globin hypersensitive site 4 (cHS4), exhibits both barrier and enhancer-blocker activity.[37] The insulator properties of the canonical 1.2-kb cHS4 can be recapitulated by a 650-bp sequence consisting of the 250-bp cHS4 core and 400 bp of sequence at its 3′ end.[37] Because the 3′ long terminal repeat (LTR) of the LV is copied and replaces the 5′ LTR upon integration into the host chromatin, the insulator sequence that is cloned within the 3′ LTR will result in the integrated LV being bordered with insulator sequences at both ends. In previous in vitro assays testing the safety of an insulated SIN-LV incorporating an MND internal promoter, we have shown that the 650-bp insulator significantly reduces transactivation of *LMO2* when placed in close proximity to the *LMO2* promoter.[27] Additionally, the insulated MND LV did not promote a pre-leukemic block in differentiation of primary murine thymocytes following transduction and in vitro culture.[38]

Our group also previously tested a series of cHS4-insulated and non-insulated SIN-LV constructs containing various internal promoters (MND, EF1α, and *WAS* 1.6-kb and 0.5-kb promoters) driving GFP reporter gene expression in a mouse gene therapy model. HSCT with LV containing the 650-bp cHS4-insulated MND-GFP (650.MND.GFP) resulted in GFP expression in all hematopoietic lineages, including platelets, that was stable over time. The 650.MND.GFP LV also showed the highest GFP expression per viral integration.[28] Therefore, based on our combined efficacy and expression data, a producer cell clone capable of generating high-titer LV with the 650-bp cHS4 insulator and MND-WASp expression cassette (650.MND.hWASp) was developed for clinical use.[27] In the current study, we utilize this clinical vector to perform an expanded efficacy and safety study. Our analysis also includes a direct comparison of LV with and without the 650-bp cHS4 insulator. Efficacy and safety was assessed in a large cohort of $Was^{-/-}$ mice, including serial transplants. We also evaluated the safety profile of these SIN-LV vectors in non-human primates (NHPs), expressing GFP instead of hWASp to improve assay sensitivity. Our combined observations strongly support future use of the insulated MND promoter for clinical WAS gene delivery.

RESULTS

650.MND.hWASp LV Efficiently Rescues WASp Expression in Affected Hematopoietic Lineages

We evaluated the ability of the insulated SIN-LV 650.MND.hWASp (Figure 1A), generated from a clinical-grade producer cell line,[27] to stably reconstitute WASp expression in the appropriate hematopoietic cell lineages using a $Was^{-/-}$ mouse gene therapy model. Expression from this LV was compared, in parallel, to the non-insulated version, MND.hWASp, that previously demonstrated reconstitution of $Was^{-/-}$ hematopoietic cell defects.[20] Lineage-depleted (Lin^-) bone marrow (BM) cells from $Was^{-/-}$ (KO) mice were transduced with SIN-LV at a MOI of 50 and transplanted into lethally irradiated $Was^{-/-}$ mice. In parallel, mock transduced $Was^{-/-}$ or C57BL/6 Lin^- BM cells were transplanted as negative (KO mock) and positive (WT mock) controls, respectively. Cells from donor mice were distinguishable from recipients by surface staining for the congenic CD45.1/CD45.2 alleles. We also performed secondary transplants to more rigorously test vector safety and to verify the reconstitution of WASp in long-term repopulating HSCs. At 12–15 weeks post-transplant, peripheral blood (PB) samples were obtained for analysis of platelets; 16 weeks post-transplant, mice were euthanized and a complete necropsy, as well as extensive phenotyping and functional assessment of hematopoietic cells within the thymus, BM, and spleen, was performed (Figure 1B). Secondary recipients were similarly assessed; however, thymus tissue was assessed only in the event that expansion of T cells was identified in the spleen or BM.

Analysis of LV-transduced donor Lin^- BM cells demonstrated an equal viral copy number (VCN) and WASp expression for both SIN-LV vectors at transplantation. WASp-expressing Lin^- BM cells were 44% and 51% (compared to 89% for WT mock) after LV MND.hWASp and 650.MND.hWASp transduction, respectively (Figure 1C). At 16 weeks post-transplant, we identified high donor engraftment levels (based on the percentage of cells congenic for the donor CD45 allele) in the BM (49%–61%) and in splenic

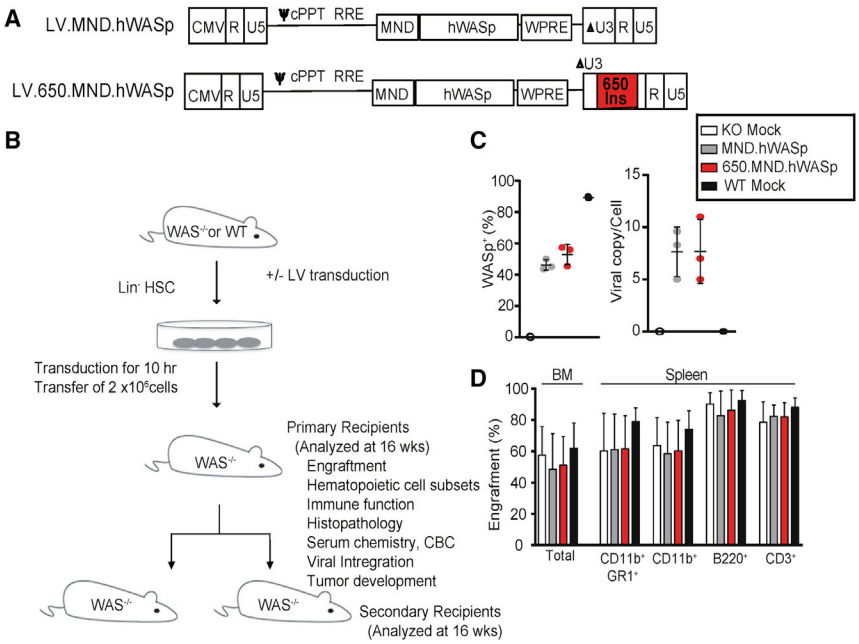

Figure 1. Evaluation of a Clinical SIN-LV for the Treatment of WAS in a Mouse Gene Therapy Model

(A) Configuration of SIN-LVs used. Expression of hWASp (with a 3′ UTR consisting of the woodchuck hepatitis virus post-transcriptional regulatory element [WPRE]) is driven by an MND promoter. Both of the 5′ long terminal repeats (LTRs) are composed of the following: a cytomegalovirus (CMV) promoter and HIV-1 R and U5 regions; the 3′ LTR of both viruses have R and U5 regions and a modified U3 region (promoter deleted; ΔU3); the insulated version (below) has a 650-bp fragment derived from the cHS4 element inserted into the ΔU3 region of the LV LTR (650 INS; red box). cPPT, central polypurine track; ψ, Psi packaging sequence; RRE, Rev response element. (B) Experimental design for in vivo studies; further details are described in the Materials and Methods. (C) Percentage of gene therapy-treated Lin$^-$ cells expressing hWASp (left) and the lentiviral copy number (VCN) per cell (right) of an aliquot of input cells cultured for 7 days. (D) Percentage of donor cells (expressing donor CD45 allele) in total BM and splenic subsets 16 weeks after transplantation with gene therapy-treated Lin$^-$ BM. Means ± SD are shown.

neutrophil (60%–78%), monocyte (59%–73%), B cell (82%–92%), and T cell (78%–88%) compartments in all treatment groups (Figure 1D).

Using a WASp-specific antibody for intracellular staining, we found that MND.hWASp and 650.MND.hWASp experimental groups exhibited WT levels of WASp expression in BM and splenic populations, including neutrophils, monocytes, B cells, CD4 and CD8 T cells, and natural killer (NK) cells (Figures 2A–2D, S1A, and S1B), with expression levels significantly increased relative to KO mock recipients. There was no statistically significant difference in the mean fluorescence intensity (MFI) of WASp intracellular staining among the two LV-treated groups (Figure S1C). Myeloid cells lack a selective advantage for WASp expression; thus, the fraction of WASp$^+$ cells at this time point likely represents the fraction of early progenitors transduced with LV.[39,40] An increase in the fraction of WASp$^+$ cells in a peripheral subset over that observed in myeloid-derived neutrophils (or monocytes) therefore implies a selective advantage for WASp$^+$ cells. In each cohort, we found that splenic B cells, CD4 and CD8 T cells, and NK cells had a significantly higher percentage of WASp$^+$ cells compared to splenic neutrophils (17% and 27% in the insulated and non-insulated LVs, respectively; solid lines in Figures 2A–2D). Interestingly, we also observed a significant increase in splenic WASp$^+$ NK1.1$^+$ CD3$^+$ cells in the 650.MND.hWASp (48%) versus the MND.hWASp (35%) experimental groups (Figure 2A), suggesting an increased selection for NK cells using the insulated LV.

We also analyzed splenic lymphocytes by surface markers that allowed us to define B and T cell sub-populations along with intracellular WASp levels (Figures 2B–2D). Our findings mostly replicated those reported previously for a non-insulated MND.hWASp LV.[20] In both gene therapy cohorts, we observed higher percentages of WASp$^+$ cells in each of the B and T cell subsets analyzed, compared to that in the myeloid compartment, indicating selection for WAS expression. Those that were statistically significant for both gene therapy cohorts were post-transitional B cells, including MZ precursors (MZps), marginal zone (MZ) and follicular mature (FM) B cells, and CD4$^+$ effector memory (T_{EM}) and regulatory (T_{Reg}) subsets. A statistically significant selective advantage for CD8$^+$ T cells was observed only in central memory (T_{CM}) and T_{EM} subsets for the 650.MND.hWASp cohort. The numerical reconstitution of splenic lymphocyte subsets was consistent with dependence on WASp expression (Figures 2E–2G): lymphocyte sub-populations where WASp expression provided selective advantage in general had increased numbers in the LV-treated cohorts. There were no significant differences in cell numbers when comparing the insulated versus non-insulated LV. Based on the above observations, we conclude that gene therapy using the 650.MND.hWASp LV rescues development of affected hematopoietic cell lineages comparably to the non-insulated vector.

A prominent finding in patients with WAS is bleeding due to a deficit in platelet numbers and function. An important consideration for WAS gene therapy then is the restoration of WASp levels in platelets.[3,4] It should be noted that the platelet defect in *Was*$^{-/-}$ mice is mild relative to that seen in human subjects, so a change in blood platelet counts was not expected.[41,42] We obtained platelets from PB 12–15 weeks post-transplantation for analysis by flow cytometry for intracellular WASp expression (Figures 2H and 2I). We found that both LVs increased the percentage of WASp$^+$ platelets relative to KO mock-treated animals. The MFI of WASp$^+$ platelets in both

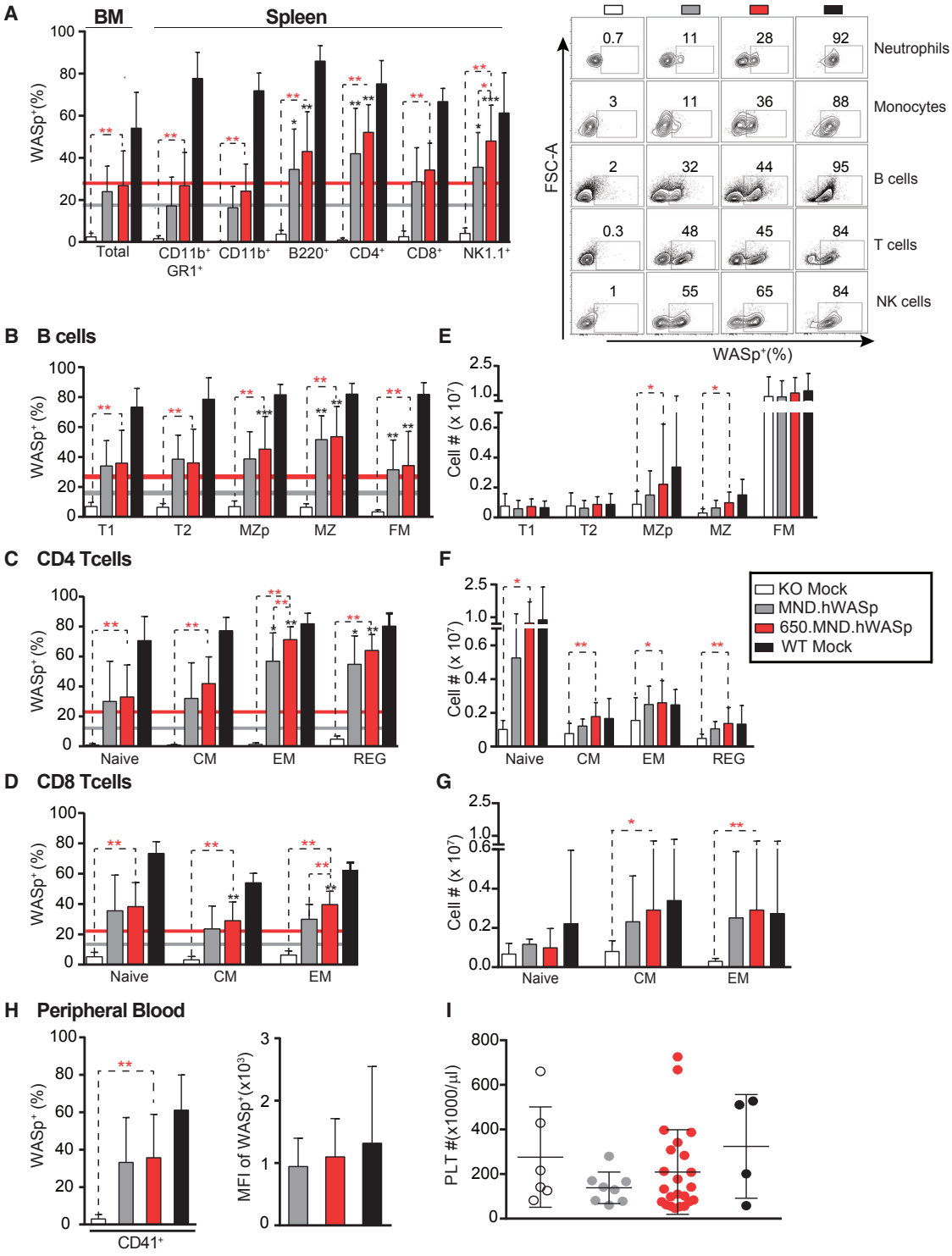

Figure 2. Restoration of WASp Expression in Affected Hematopoietic Lineages following LV Gene Therapy in WAS$^{-/-}$ Primary Recipient Mice

Shown are the proportion of WAS^{+} cells and numerical reconstitution of lymphocytes and platelets 16 weeks post-transplant. (A) WASp-expressing cells in total BM and in hematopoietic lineages of the spleen. Colored horizontal lines in this and subsequent panels show the average percentage of WASp^{+} splenic neutrophils (CD11b^{+} GR-1^{+}) in the MND.hWASp-treated (gray) and 650.MND.hWASp-treated (red) cohorts for comparison. The right panel shows representative flow cytometry analysis of splenocytes. (B–D) WASp^{+} cells within developmental subsets of splenic B (B) and T cells (C and D). B cells are plotted in order from least to more mature subsets: transitional 1 (T1),

(legend continued on next page)

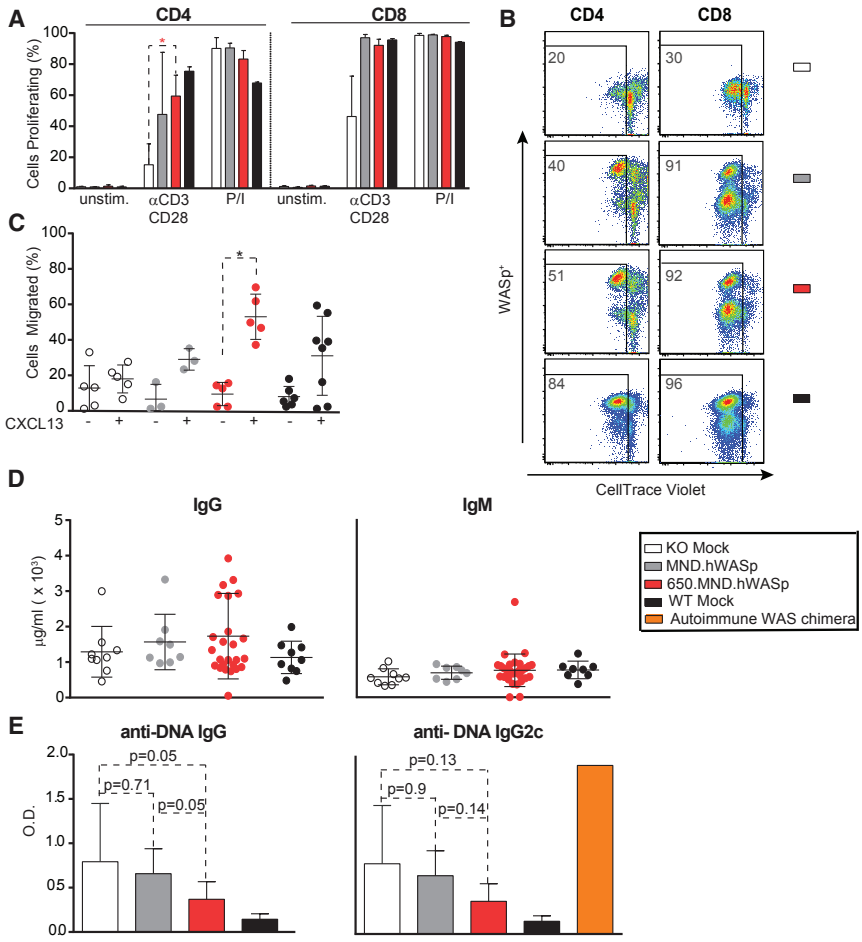

Figure 3. Reconstitution of Immune Cell Functions following LV Gene Therapy in Primary Recipients

Assays of immune cell function 16 weeks after BM transplantation. Bars show the mean ± SD. (A) The percentage of cells that underwent ≥1 cell division 72 hr after incubation with CD3/CD28 antibodies or P/I (as measured by CellTrace Violet dilution). Shown are cells within CD4 (left) or CD8 (right) staining gates by flow cytometry. Data are from one of the three independent experiments: n = 3 (KO and WT mock, MND.hWASp) and 5 (650.MND.hWASp). (B) Flow cytometry analysis showing CellTrace Violet labeled splenocytes 72 hr post-CD3/CD28 stimulation, gated on live and either $CD4^+$ or $CD8^+$ populations. Numbers indicate the percentages that have proliferated after CellTrace Violet labeling. (C) B cell ($CD43^-$ splenocyte) migration in response to media only (–) or media supplemented with CXCL13 chemokine (+). Each dot indicates the percentage of B cells from a single mouse that migrated through the 5-μm-pore transwell. Data are from two independent experiments: n = 5 (KO mock, 650.MND.hWASp), 3 (MND.hWASp), and 8 (WT mock). (D) IgG and IgM and (E) anti-double-stranded DNA antibody levels in the serum of primary recipients as determined by ELISA 16 weeks post-transplant. Data are from three independent experiments: n = 5 (KO and WT mock), 4 (MND.hWASp), 2 (WT) (D only), and 12 (650.MND.hWASp). Serum from an autoimmune WAS chimera[21] (E only) with high serum anti-DNA antibodies was used as a positive control. The p value was determined by unpaired two-tailed t test. *p < 0.024.

gene therapy cohorts was similar to that of wild-type platelets, confirming the ability of the MND promoter to drive efficient transgene expression in this lineage.

650.MND.hWASp LV Promotes Reconstitution of Immune Cell Functions

Improvement in T Cell Receptor Signaling

WASp has a role in actin polymerization downstream of the T cell receptor (TCR)[6] and its loss impacts TCR responses including proliferation of murine CD4 T cells.[41,42] Note that CD8 T cell TCR responses are only partially impacted by the loss of WASp. We tested the proliferation of murine splenic T cells in vitro in response to anti-CD3 and anti-CD28 stimulation (αCD3/28), read as dilution of CellTrace Violet (a fluorescent succinimidyl ester dye) from stained cells by flow cytometry. As expected, KO mock $CD4^+$ T cells proliferated minimally in response to αCD3/28, while a substantial fraction of those from LV-treated or WT cohorts had proliferated by 72 hr. The percentage of cells that had proliferated at this time point was not significantly different between the two SIN-LV treatments. We consistently found that $Was^{-/-}$ $CD8^+$ T cells proliferated in response to TCR stimulation even without gene therapy treatment, but LV treatment increased the overall proportion of cells proliferating in response to CD3 (Figures 3A and 3B). Control $CD4^+$ and $CD8^+$ T cells from all treatment groups proliferated equally well in response to phorbol 12-myristate 13-acetate (PMA)-ionomycin (P/I), which activates the TCR signaling pathway downstream of WASp.

Restoration of B Cell Motility

Contrary to T cells, WASp deficiency renders B cells hyper-responsive to antigen receptor stimulation.[21,43] However, WASp deficiency

transitional 2 (T2), marginal zone precursor (MZP), marginal zone (MZ), and follicular mature (FM). T cell subsets are designated as naive, central memory (CM), effector memory (EM), or regulatory (REG). (E–G) Absolute number of specific developmental subsets of splenic B cells (E) and $CD4^+$ (F) or $CD8^+$ (G) T cells. (H) Percentage (left) and MFI (right) of $WASp^+$ platelets in PB. (I) Number of platelets per microliter of PB. Bars and error bars represent the mean ± SD. In (A)–(D) and (H), n = 10 (KO mock, MND.hWASp), 28 (650.MND.hWASp), and 9 (WT mock) from three independent experiments. In (E) to (G), n = 3 (KO and WT mock), 5 (MND.hWASp), and 12 (650.MND.hWASp) from one experiment. In (I) n = 4 (WT mock), 7 (KO mock), 8 (MND.hWASp), and 22 (650.MND.hWASp) from one experiment. *p < 0.04, **p < 0.002, ***p < 0.0001. Asterisks in red indicate p values of comparisons indicated by the dashed lines; asterisks in black show p values comparing the mean value indicated with that of the monocytes (gray or red horizontal line) in the same cohort, to test the significance of selective advantage.

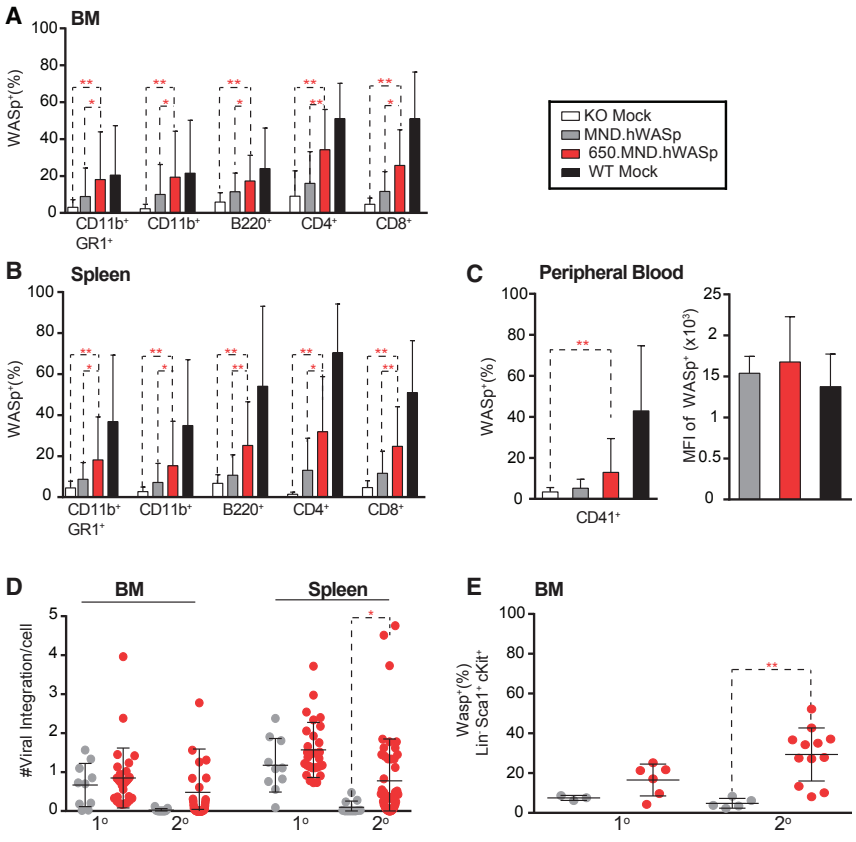

Figure 4. Maintenance of VCN and WASp⁺ Expression in HSC and Their Progeny in 650.MND.hWASp LV-Treated Animals following Secondary Transplantation

Proportion of WASp⁺ cells in the BM (A) and spleen (B) and in PB platelets (C) of secondary recipients (16 weeks post-transplantation with BM from primary recipients). Data represent three individual experiments: n = 12 (KO mock), 16 (MND.hWASp), 51 (650.MND.hWASp) (n = 50 in C), and 15 (WT mock). In (C), the percentage (left) and MFI (right) of WAS⁺ platelets is shown. (D) Comparison of viral copy number (VCN) determined by qPCR of gDNA extracted from total BM and splenic cells of primary (1°) and secondary (2°) recipient mice; each dot represents a single animal. Data are from three independent experiments for both primary (n = 10 for MND.hWASp and n = 28 for 650.MND.hWASp) and secondary recipients (n = 16 for MND.hWASp, 51 for 650.MND.hWASp). (E) Percentage of WASp⁺ cells in HSCs in BM of primary (1°) and secondary (2°) gene therapy recipients. Data represents two unique experiments for both primary (n = 3 for MND.hWASp and n = 6 for 650.MND.hWASp) and secondary recipients (n = 6 for MND.hWASp and 12 for 650.MND.hWASp). In all panels, the mean ± SD value is shown. p values were calculated using the unpaired two-tailed t test. *p < 0.04, **p < 0.005.

impacts B cell motility and homing in response to chemotactic agents, ultimately affecting B cell development and selection.[44] To determine whether SIN-LVs corrected this motility defect, we measured the number of total splenic B cells (CD43-depleted splenocytes) migrating across a transwell membrane into media with or without the chemokine CXCL13. For both gene therapy cohorts, the addition of CXCL13 increased the percentage of B cells migrating across the transwell membrane (Figure 3C). A significantly higher fraction of B cells from the 650.MND.hWASp LV cohort migrated relative to KO mock B cells, and this was comparable to the fraction of WT B cells that had migrated. Thus, 650.MND.hWASp LV rescues the homing defect in *Was*$^{-/-}$ B cells.

Reduction in Autoantibody Production

In the presence of WASp-expressing T cells, WASp-deficient B cells trigger spontaneous germinal center responses that lead to autoantibody production and autoimmune disease in mice.[21–23] These findings are likely to explain the increased rates of autoimmune disease in human patients with WAS with low-level donor chimerism following HSCT.[9] As quantified by ELISA in this study, we found that total serum immunoglobulin G (IgG) and IgM levels were similar across treatment groups (Figure 3D). In contrast, there was a trend for reduced anti-DNA autoantibodies present in KO mock recipients (assessed as total IgG or by the pathogenic IgG2c subclass) in MND-LV-treated cohorts, approaching levels present in WT mock in 650.MND.hWASp LV-treated mice (Figure 3E). These findings suggest that 650.MND.hWASp LV drives WASp expression at levels that may limit the subsequent risk for autoimmune disease.

Sustained 650.MND.hWASp LV Marking and Expression following Serial Transplantation

Secondary transplants were performed to determine whether 650.MND.hWASp targeted long-term repopulating HSCs and to test relative safety.[45,46] BM cells from each primary recipient (16 weeks post-primary transplant) were transplanted into two irradiated secondary recipients (10×10^6 cells/recipient). We performed extensive analysis of the secondary recipients at week 16 by flow cytometry, histology, hematology, and clinical chemistry. Compared to primary donors, secondary recipients from all donors (including WT mock controls) had a smaller proportion of WASp⁺ cells within the myeloid, B cell, and T cell compartments in the BM and spleen (Figures 4A and 4B). Interestingly, secondary recipients from the 650.MND.hWASp group had higher proportions of WASp⁺ cells compared to the MND.hWASp group in hematopoietic lineages of the BM (Figure 4A) and spleen (Figure 4B). Additionally, only the insulated LV improved WAS expression in platelets (Figure 4C), although for both vectors, platelets that did express WASp did so at equivalent levels (MFI) to those from the WT mock cohorts. We next determined the average VCN by qPCR in total splenocytes and BM from primary and secondary recipients (16 weeks after their respective BM transplants; Table 1). In primary recipients, the

Table 1. Safety Parameters of Pre-clinical LV Gene Therapy

LV	Total No. of Mice	VCN (Mean ± SD)		No. with Malignancy Derived from			No. of Deaths (<4 Weeks Post-transfer)
		Spleen	BM	Donor	Recipient	Unknown	
Primary							
KO mock	10	0	0	0	0	0	0
WT mock	9	0	0	0	0	1	0
MND.hWASp	10	1.17 ± 0.21	0.66 ± 0.17	0	0	0	0
650.MND.hWASp	32	1.15 ± 0.13	0.84 ± 0.14	0	1	0	3
Secondary							
KO mock	16	0	0	0	0	0	2
WT mock	19	0	0	0	0	0	0
MND.hWASp	14	0.09 ± 0.04	0.02 ± 0.01	0	3	0	0
650.MND.hWASp	56	0.77 ± 0.15	0.43 ± 0.16	0	2	2	3

average VCN per cell was increased in the splenic compartment relative to the BM, reflecting positive selection of $WASp^+$ lymphocytes (Figure 4D), and the differences between the two LV groups were not statistically significant. The VCN within the BM of secondary recipients was lower than that of the primary recipients, but again increased in the spleen. Notably, 650.MND.hWASp LV-treated secondary recipients exhibited a significantly higher VCN within the spleen and a larger proportion of $WASp^+$, Lin^- HSCs within the BM compared to animals treated with MND-hWASp LV (Figures 4D and 4E, respectively). These combined findings imply that inclusion of the insulator exerts a significant impact by allowing stable WASp transgene expression, thus providing a selective advantage to cells with the insulated WASp transgene.

Assessing the Safety of 650.MND.hWASp LV Gene Therapy

Mice transplanted with 650.MND.hWASp SIN-LV-treated cells (either as primary or secondary transplants) had no statistically significant change in survival rates compared with the other gene therapy cohorts (Figures 5A and 5B). Table 1 summarizes the mortality and morbidity events occurring in the course of this study. Of 61 primary transplanted mice, three died from unknown causes within 4 weeks of their transplant, all from the larger 650.MND.hWASp LV cohort. Note that 32 of the primary recipient mice received 650.MND.hWASp LV gene therapy; the other 29 were divided into the remaining three cohorts. Mortality events occurring within 4 weeks post-transplant are likely to be due to the conditioning regimen, and the rates they occurred in this study as a whole are lower than those historically seen in previous LV gene therapy models we have performed (7%), although the rate for the insulated LV group alone (9.4%) is higher. At the 16-week study endpoint, we identified two mice with thymic lymphomas: one received 650.MND.hWASp gene therapy-treated cells (mouse 19), and the other received WT mock cells (mouse 36). The $CD4^+CD8^+$ lymphoma of mouse 19 was identified both by flow cytometry and by histopathology of thymus and spleen (Figure 5C). Using flow cytometry and antibodies specific to donor and recipient congenic markers, we determined that this lymphoma was recipient derived (Figure 5D); consistent with this conclusion, there were no viral integrations (by qPCR) within genomic DNA (gDNA) obtained from thymic tissue of this mouse (Table 2). Mouse 36 from the WT mock cohort developed a thymic lymphoma identified during histopathology screening but not detected by flow cytometry analysis. We were unable to determine whether this tumor was donor or recipient derived using congenic antibodies. Flow cytometry of harvested hematopoietic tissues and extensive histological analysis post-transplantation did not reveal evidence of clonal expansion within any of the other primary transplant recipients. Complete blood counts (CBCs) and serum chemistries of PB were identical between the treatment groups, except for one of the mice with lymphoma (mouse 19; Figures S2 and S3).

The lifespans of secondary recipients were not significantly different than those of the primary recipients. Five of the 105 secondary recipients died within 4 weeks of the transplant procedure from unknown causes: three of these mice were from the 650.MND.hWASp gene therapy cohort, and two were from the KO mock cohort (Table 1). At the 16-week endpoint, we identified five secondary transplanted mice with clonal expansion of T cells by flow-based phenotyping (Table 2): two were from the 650.MND.hWASp cohort and consisted of recipient-derived (based on congenic markers and lack of VCN) $CD4^+CD8^+$ (mouse 116) and $CD8^+$ (mouse 155) T cells; three animals in the MND.hWASp cohort (mice 68, 69, and 128) developed $CD4^+CD8^+$ recipient-derived lymphomas (and also had abnormal hematological and clinical chemistries; Figures S4 and S5). We identified two additional probable lymphomas by histological analyses (not detected by flow cytometry) within the 650.MND.hWASp gene therapy group (mice 111 and 153). Because these tumors were identified only by histopathology, after tissue was fixed and embedded, VCN and congenic marker expression could not be assessed.

A variety of radiation-associated lesions were identified during histological examination (Table S1); these were uniformly distributed across all groups. The prevalence of recipient-derived lymphomas in this WAS gene therapy model is consistent with the oncogenicity

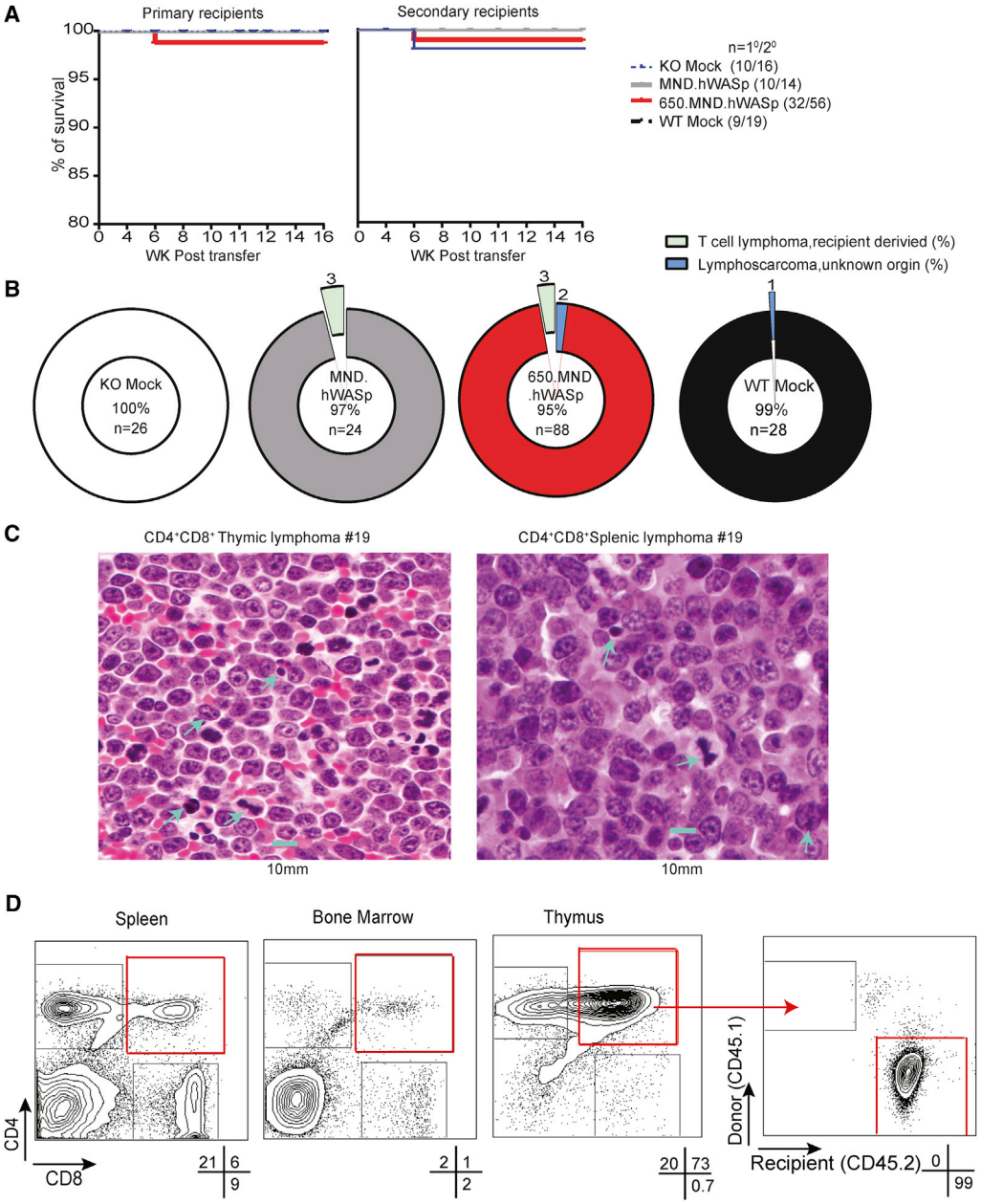

Figure 5. Overall Survival and Absence of Donor-Derived Malignancies in LV-Treated Mice

(A) Kaplan-Meier survival curves for primary (left) and secondary (right) recipients during the 16-week post-BM transplant periods. (B) Pie chart showing tumor incidence as a percentage of all (primary and secondary) recipients from each treatment cohort. The percentage of mice with no tumors is shown in center of each chart. (C) Hematoxylin and eosin-stained sections of thymus and spleen of a secondary recipient from the 650.MND.hWASp cohort with a host-derived $CD4^+CD8^+$ lymphoma at ×60 magnification. The scale bar represents 10 μm. Blue arrowheads point to mitotic figures. (D) Flow cytometry plots of cells from the affected mouse shown in (C). Shown are CD4 and CD8 surface expression in indicated tissues. The recipient's tumor origin was identified by congenic marker stain after gating on $CD4^+CD8^+$ thymic cells (plots at right). Percentages of live cells within each gate are indicated beneath the plots.

of the conditioning regimen in a genetically susceptible immunodeficient ($Was^{-/-}$) mouse in the C57BL/6 background.[46] Overall, we found no evidence of clonal toxicity associated with integration of the 650.MND.hWASp LV in this extensive pre-clinical study.

MND Promoter-Based LVs Exhibit Robust Expression and Polyclonal Hematopoiesis in a NHP Gene Therapy Model

To assess the safety and the integration profile of SIN-LV with various internal promoters in a large animal model, we performed gene

Table 2. Features of Malignancies Found in Experimental Mice

	Flow Cytometry				
LV (Mouse Number)	Phenotype	Donor (%)	Recipient (%)	Histopathology	VCN
Primary Recipient					
WT Mock (36)	ND	ND	ND	+ (thymus, lungs)	ND
650.MND.hWASp (19)	$CD4^+CD8^+$	0	93.8	+ (multiple organs)	0
Secondary Recipient					
650.MND.hWASp (116)	$CD4^+CD8^+$	0	99.7	+ (multiple organs)	0
650.MND.hWASp (155)	$CD8^+$	0	99.5	+ (multiple organs)	0
650.MND.hWASp (111)	ND	ND	ND	+ (thymus, lungs)	ND
650.MND.hWASp (153)	ND	ND	ND	+ (thymus)	ND
MND.hWASp (68)	$CD4^+CD8^+$	0	99.8	ND	0
MND.hWASp (69)	$CD4^+CD8^+$	0	99.8	ND	0
MND.hWASp (128)	$CD4^+CD8^+$	0	99.4	ND	0

ND, not determined.

therapy in healthy juvenile pigtailed macaques (*Macaca nemestrina*) using a $CD34^+$ autologous HSC myeloablative transplant protocol.[47] Similar to our mouse gene therapy studies,[39] we first compared the efficacy and safety of LV containing either the human 1.6-kb *WAS* promoter (WS1.6; currently in use in clinical trials)[10,12] or the MND promoter (Figure 6A). In a competitive repopulation experiment, $CD34^+$ BM cells were separately transduced with WS1.6. GFP or MND.YFP SIN-LV. Equivalent numbers of marked cells (7.2×10^6 $CD34^+$ cells from each transduction/kg; total of 14.4×10^6/kg body weight) were infused into animal F09002 following 1,020-cGy total body irradiation. PB samples demonstrated hematopoietic recovery and engraftment of gene-modified cells within 3 weeks following transplant and stable CBCs and serum chemistries over a >30-month follow-up period (Figures S6 and S7). Initial flow cytometry showed gene-modified cell levels of ~30% and ~15% for the MND (yellow fluorescent protein [YFP^+]) and WAS1.6 (GFP^+) promoter-encoding LV-transduced cells among PB leukocytes, and these values were stably maintained for more than 1,000 days (Figure 6B). We observed stable granulocyte and lymphocyte marking up to the latest time point of follow-up (1,153 days), with 38.7% YFP^+ and 15.6% GFP^+ granulocytes and 27.0% YFP^+ and 15% GFP^+ lymphocytes (data not shown). We also observed a marked increase in the MFI for YFP^+ cells compared to GFP^+ cells (Figures 6C and 6D), consistent with the robust expression expected from the MND promoter compared to the WAS1.6 promoter.[20]

To assess the diversity of clonal contributions to this pool, we performed high-throughput retroviral integration site (RIS) analysis on flow-sorted YFP^+ and GFP^+ PB leukocytes 502 and 1,153 days post-transplant. Modified genome sequencing (MGS)-PCR of gDNA from sorted cells was used to determine genomic sites of provirus integration.[48] We observed highly diverse integration sites in all samples assayed, with distinct clonal contributions in each transduced cell population (Figure 6E). In total, we identified 4,699 and 1,688 unique integration sites of the YFP^+ and GFP^+ LVs, respectively. The most abundant clone constituted 1.5% (YFP^+) and 3.7% (GFP^+) of the integration site sequences identified, implying a highly polyclonal expansion of progenitors. We identified a higher number of distinct clones in the YFP^+ cell population, suggesting that increased gene marking in this population is not due to expansion of a single or small number of clones. RISs were mapped on all chromosomes, and comparison of the global genomic distribution of integration sites in these samples (Figure 6F) showed no promoter-specific changes in distribution pattern. This animal displayed no evidence for adverse events at nearly 4 years post-transplantation, and gene marking remained stable.

Owing to the correlation between retroviral promoter activity and insertional mutagenesis observed in γ-retrovirus-mediated gene therapy trials for both X-SCID and WAS,[13–15] we next tested whether inclusion of a chromatin insulator in the MND promoter SIN-LV could improve safety while maintaining efficient gene transfer, engraftment, and clonal diversity in this animal model. We performed a three-arm competitive repopulation assay (Figure S8A) using $CD34^+$ cells transduced with either cHS4.MND.GFP (using the 1.2-kb full-length chicken β-globin insulator element), 650.MND.mCherry, or 400.MND.BFP (an ~400-bp insulator fragment).[37] We observed only small differences in in vitro transduction efficiency of $CD34^+$ cells between the three LV vectors (38% GFP^+, 23% $mCherry^+$, and 35% blue fluorescent protein [$BFP]^+$). Transduced cells were transplanted into the autologous myeloablated animal A11207 (3.5, 4.3, and 2.9×10^6 transduced cells/kg for cHS4.MND.GFP, 650.MND.mCherry, and 400.MND.BFP SIN-LVs, respectively; total of 10.7×10^6 $CD34^+$ cells/kg of body weight). The transplanted animal demonstrated hematopoietic recovery and engraftment of gene-modified cells within 1 week after transplant. All three arms engrafted equivalently, as evidenced by the levels of each fluorescent protein in PB. This sustained expression and gene marking supported stable

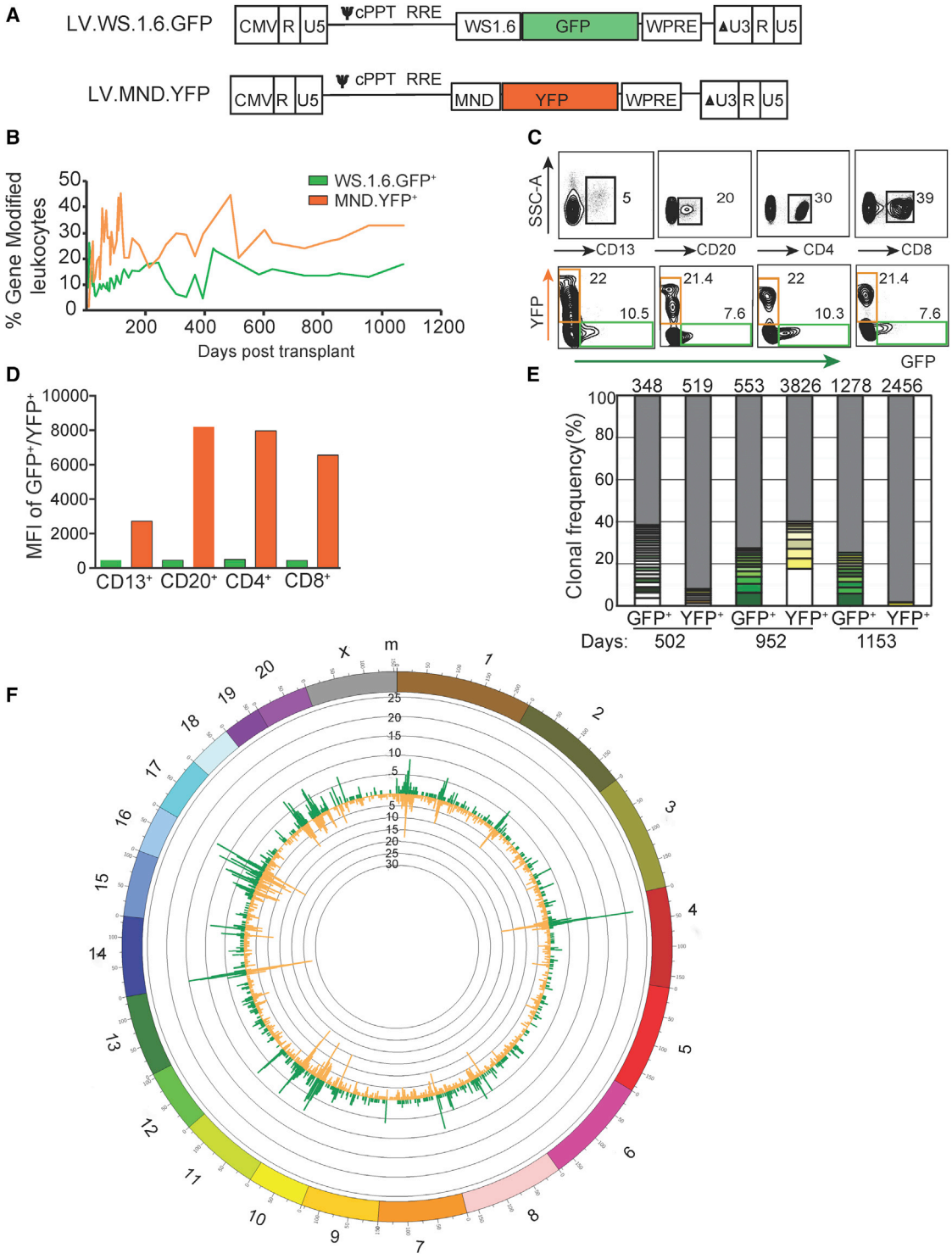

Figure 6. Stable Promoter Activity and Polyclonal Hematopoiesis Using the Non-insulated MND LV in a Long-Term NHP Gene Therapy Model

(A) Schematic diagram of SIN-LV used in competitive repopulation study performed with NHP autologous BM, GFP, yellow fluorescent protein (YFP), and the 1.6-kb proximal human *WAS* promoter (WS1.6).[57] (B) Percentage of cells expressing the indicated fluorescent protein in peripheral blood mononuclear cells (PBMCs) over time after transplant. (C) Representative flow plots showing marking (bottom row) within specific PB subsets (top row) obtained 326 days post-transplant. (D) The MFI for each sub-population in this sample is shown. (E) Frequency of MSG-PCR clones identified in sorted GFP$^+$ or YFP$^+$ PB cells at 502, 952, or 1,153 days after transplant. The total number

(legend continued on next page)

hematopoiesis in this animal for nearly 2 years with no adverse events (Figures S6–S8B). Stable granulocyte and lymphocyte marking was observed up to the latest time point of follow-up (782 days), with 1.5% GFP$^+$, 1.4% mCherry$^+$, and 0.9% BFP$^+$ granulocytes and 0.9% GFP$^+$, 0.4% mCherry$^+$, and 1.7% BFP$^+$ lymphocytes (data not shown).

To assess the diversity of clonal contributions to this pool, we collected PB and BM at approximately the same time point after transplant (days 221 and 223 post-transplant for PB for BM, respectively) and we used fluorescence-activated cell sorting (FACS) to sort PB leukocytes by fluorescent protein expression to distinguish between the three insulator elements. CD34$^+$ leukocytes from the BM were also purified to correlate clonal contributions observed in the PB fluorescent protein-sorted populations. RIS analysis of gDNA isolated from sorted and purified cells was then performed by MGS-PCR. Highly diverse integration sites were observed in all samples assayed, with distinct clonal contributions in each transduced cell population (Figure S8C). We identified 265–392 unique RISs for sorted GFP, mCherry, and BFP $^+$ PB leukocytes and 396 unique RISs in total BM CD34$^+$ cells. There were no significant differences in the number of clones observed for each sample, which is consistent with the similar levels of gene marking in each cell population. We identified a total of six clones in the BM CD34$^+$ cell population that were also identified in one of the three PB fluorescent protein-sorted populations, demonstrating the contribution from a CD34$^+$ cell residing in the BM to a marked PB leukocyte. Of these, three were GFP$^+$ (full-length insulator), two were mCherry$^+$ (650-bp insulator), and one was BFP$^+$ (400-bp insulator). Of the CD34$^+$ BM clones identified, the two most prevalent contributors were both from the GFP$^+$ lineage (full-length insulator).

After establishing the genomic positions of all LV integration sites for both animals (F09002 and A11207), we compared their positions to the 2010 rheMac3 RefSeq gene list available from the UCSC Genome Browser using a custom python script.[49] For each insertion site, we determined the distance to the nearest transcription start site (TSS) relative to the direction of transcription (Figures S9A and S9B) and gene name. If the insertion fell within a gene, the gene name and genomic feature (i.e., within an intron, etc.) were recorded. In both animals F09002 and A11207, we observed an equivalent number of integration events within 100 kb of TSS regardless of the promoter (F09002) or insulator element (A11207) tested. For animal A11207, genes proximal to the integration sites identified at 96, 221, and 392 days after transplant were compared to the established list of oncogenes from the Cosmic Cancer Gene Database (http://cancer.sanger.ac.uk/cosmic) (Table S2).[50] Of 21 integrations identified, all were within unique proto-oncogenes; only one identical integration was found at two time points (96 and 392 days post-transplant; FBXW7, F-Box and WD repeat domain containing 7, E3 ubiquitin protein ligase). The integration was 69.4 kb downstream of the transcription start site of this tumor suppressor gene, within intron 3. The contribution of this clone was <0.1% of overall hematopoiesis at both time points, implying a lack of a biological impact from this integration during this time period. Together, these data support the transduction efficiency, engraftment, and clonal diversity of insulated LV vector-transduced autologous CD34$^+$ hematopoietic cells in the clinically relevant non-human primate animal model, without evidence of insertional mutagenesis.

DISCUSSION

Here we report evidence of long-term efficacy and safety of an SIN-LV with an insulated MND internal promoter for WAS gene therapy in *Was*$^{-/-}$ mice and for a non-human primate model using a reporter gene. In primary recipient *Was*$^{-/-}$ mice, we found similar features of restored immune cell function in both gene therapy cohorts (650.MND.hWASp and MND.hWASp), including stable engraftment of WASp-expressing cells in all hematopoietic lineages examined; progressive selection for WASp$^+$ cells among T, NK, and B cell lineages; correction of T and B cell development and function; and restoration of wild-type levels of WASp expression in platelets. These findings expand upon those of a previous murine gene therapy study using a non-insulated MND.hWASp SIN-LV that used a different LV backbone than used here.[20] In the current study, mice receiving the insulated 650.MND.hWASp gene therapy also exhibited a trend for lower levels of autoimmune-associated anti-DNA autoantibodies of the IgG and IgG2c subtypes compared to animals treated with the non-insulated LV construct.

In our murine gene therapy experiments, serial BM transfers into secondary *Was*$^{-/-}$ recipients were performed to verify long-term hematopoietic stem cell (LT-HSC) transduction and long-term efficacy of the viral vectors, and to increase the sensitivity of detecting vector-induced transformation events in vivo.[45] We found that the 650.MND.hWASp gene therapy vector resulted in superior immune cell reconstitution in the secondary recipients compared with the non-insulated MND.hWASp LV, including significantly higher percentages of WASp$^+$ immune cells in BM, spleen, and PB. Additionally, although the number of viral integrations per cell in BM and splenic cells of primary recipients were similar for both LV gene therapy cohorts, both the number of viral integrations and WASp expression in HSCs and progeny was significantly higher in 650.MND.hWASp-treated secondary recipients by the 16-week experimental endpoint. These striking observations are consistent with the interpretation that the insulated vector more effectively prevents epigenetic silencing in transduced long-term repopulating HSCs. In this scenario, higher-level WASp expression in donor HSCs (derived from primary recipients) is predicted to facilitate

of clones sequenced is indicated at the top of each bar in the chart. Thickness of bar segments indicates the frequency of a particular clone; the color given to each clone is consistent for comparison between time points. (F) Circos plot mapping RIS positions identified in GFP$^+$ (green histogram) and YFP$^+$ (yellow histogram) PB cells (obtained between 502 and 1,153 days after gene therapy) to the *Rhesus* genome (outer circle showing chromosome numbers). The *Rhesus* genome was divided into 1-Mbp bins; the heights of the histograms indicate the number of integrations found in a 1-Mbp bin.

increased competitive repopulation in secondary recipients, an outcome that would also promote the observed selective expansion of $WASp^+$ differentiated lymphoid subsets in 650.MND.hWASp secondary recipients. This idea is supported by previous work showing that migration defects in WASp-deficient HSCs hamper long-term hematopoietic reconstitution in a competitive repopulation setting.[51] Together, these findings strongly imply that inclusion of the 650-insulator element is likely to improve sustained expression in LT-HSCs in a clinical application.

There were no statistically significant differences in survival rates between treatment groups in this study. Despite large cohorts receiving gene therapy-treated HSCs (42 primary and 70 secondary transplant recipients), six incidences of clonally expanded cells were identified by flow cytometry at autopsy (one primary and five secondary recipients); all originated from recipient progenitor cells, with no viral integrations detected by PCR. In addition, three cases of thymic lymphoma, including two in the secondary 650.MND.hWASp LV and one in the primary WT mock treatment groups, were identified based only on detailed examination of histological sections. While we were unable to definitively determine whether these latter tumors were donor or recipient derived, this rate of lymphoma development is consistent with our previous baseline observations in WAS-deficient recipient mice.

Compared with mice, large animal gene therapy trials more closely model the number of transduced LT-HSCs that must be transplanted into a human subject, as well as their higher proliferative demands over a longer time span.[52] Because of the close genetic relationship between humans and NHPs, NHP HSCs respond to many of the recombinant human cytokines and other reagents used for clinical mobilization, selection, culture, transduction, and myeloablative total body irradiation (TBI).[52,53] In order to directly compare expression from two different internal promoters in the same animal, we used fluorescent reporter genes (GFP and YFP) transferred using SIN-LV gene therapy of BM from a pigtailed macaque, followed by autologous transplantation. Here we found that the proportion of cells in the periphery expressing either fluorescent protein was stable over 3 years. However, expression from the MND promoter was evident in a higher proportion and at a higher MFI in PB cells of all cell lineages compared with that of the WS1.6 promoter. Using a similar strategy in a second pigtailed macaque gene therapy experiment, we were able to simultaneously test three different fragments of the canonical 1.2-kb cHS4 insulator (upstream of the MND-fluorescent protein cassette) for their ability to prevent clonal dominance. As suggested by in vitro assays, insertional mutagenesis was not detected even after 2 years, and engraftment remained polyclonal with no evidence of clonal dominance (i.e., no individual clonal contribution of >20% to the total pool identified). These data imply that increased expression elicited by the viral MND promoter over the WS1.6 promoter in the context of a SIN lentivirus vector does not compromise transduction efficiency or clonal diversity of autologous $CD34^+$ hematopoietic cells in the clinically relevant non-human primate animal model.[28]

Although there was no change in the level of engrafted gene-modified cells as a function of the different insulator elements used, inclusion of an insulator may reduce overall engraftment levels when the number of gene-modified PB leukocytes is compared between animals F09002 and A11207. Finally, although the non-insulated MND promoter showed insertional transactivation when inserted proximal to the LMO2 locus in Jurkat T cells by Cre-mediated cassette exchange and in a previous murine study,[20,28] we found no evidence for toxicity in our murine or NHP studies, suggesting that these animal models, as has been previously noted,[46,54] may lack the sensitivity to distinguish between LV vectors with low rates of genotoxic events.

Together, these studies suggest that the use of an insulated SIN-LV vector incorporating an MND internal promoter may strike a necessary balance for WAS gene therapy: driving sufficient expression of WASp to stably restore the immune cell deficits of WAS and WT levels of WASp expression in platelets while minimizing the potential of integrated proviral cassettes to create transactivational mutagenesis. Furthermore, our observations regarding the capacity of this vector to reconstitute both lymphocyte function and WASp expression in platelets strongly support consideration of the 650.MND.hWASp SIN-LV for clinical gene therapy trials for the treatment of WAS. Finally, our data suggest that use of insulated SIN-LV vectors harboring MND internal promoter expression cassettes may be considered for other hematopoietic disorders in which sustained high-level transgene expression in multiple lineages is required to achieve developmental and/or functional reconstitution.

MATERIALS AND METHODS

Viral Vectors

The SIN-LV backbone pCL20cw has been described previously.[55,56] Plasmid pCL.HS4 has the full 1.2-kb HS4 insulator element from the chicken β-globin locus[37] inserted into the 3′ U3 region of the viral LTR of pCL20cw. pCL400 contains 400 bp of the insulator sequence from the 3′ end of the 1.2-kb insulator fragment, while pCL650 has 650 bp of the insulator (comprising the 250-bp core and 400 bp from the 3′ end of the 1.2-kb insulator fragment) integrated into the 3′ LTR. We used the MND promoter[26] as the internal promoter driving transgene expression in all vectors except pCL.WS1.6.GFP, which instead uses the 1.6-kb human *WAS* promoter to drive GFP expression.[57] cDNA encoding human WASp was inserted downstream of the MND promoter in a pCL650 backbone to generate pCL650.MND.WASp, and WASp was replaced by GFP to make pCL650.MND.GFP. pCL.400,MND.mCherry had the coding region for mCherry in a pCL400 backbone and pCL.MND.YFP was created by insertion of an MND.YFP cassette into the pCL backbone without any insulator element. Third-generation LV stocks were generated by transient transfection of HEK293T cells with the vector plasmid, pCAGkGP1.1R (packaging), pCAG4-RTR2 (rev), and pCAG4 VSVG (envelope) plasmids.[58,59] Forty-eight hours post-transfection, the viral supernatant was filtered through a 0.22-μm filter and centrifuged at 8,500 × *g* overnight at 4°C. The virus was suspended in

Hank's balanced salt solution to achieve a 100-fold concentration, then stored at −80°C. LV stocks for pCL.650.MND.WASp were generated from a Tet-regulated version of the same (TL-CL.650.MND.WASp) by transfection of ligated vector concatamers into GPRT-G helper cells as described previously.[27] LV titers were determined by infection of NALM-6 cells with serial dilutions of viral stocks and detection of proviral sequences by qPCR. Viral titers were calculated as proviral integrations using a standard curve generated from gDNA of a NALM-6 clone with a single copy of integrated provirus.[60]

Murine Lin⁻ BM Transduction and Transplantation

Strains of mice used were C57BL/6 (WT), *Was*$^{-/-}$ (B6:129-*Was*^{tm1Sbs} crossed into the C57Bl/6 background for nine generations[41]), and WT and *Was*$^{-/-}$ strains that were cross-bred with B6.SJL-*Ptprc*^{a} *Pepc*^{b}/BoyJ (Jackson Laboratories) for congenic marking with the CD45.1^{+} (*Ptprc*^{a}) allele (C57BL/6 mice have the CD45.2^{+}/*Ptprc*^{b} allele). Mice were maintained in a specific pathogen-free facility at the Seattle Children's Research Institute (SCRI). All studies were performed according to the Association for Assessment and Accreditation of Laboratory Animal Care (AAALAC) standards and were approved by the SCRI Institutional Animal Care and Use Committee (IACUC).

Methods for collection and LV transduction of murine Lin^{-} BM, and transplantation of LV-treated cells into irradiated recipients, were similar to those previously described.[20,60] BM cells isolated from euthanized 6- to 8-week-old donor mice (WT or *Was*$^{-/-}$; congenically marked either CD45.1^{+} or CD45.2^{+}) were enriched for lineage-negative cells using the EasySep Mouse Hematopoietic Progenitor Cell Enrichment Kit (StemCell Technologies). Lin^{-} cells (4×10^{6} cells/mL) in HSC media (StemSpan SFEM; StemCell Technologies) with murine stem cell factor (SCF) and thrombopoietin (50 and 20 ng/mL, respectively) were transduced without (mock) or with LV at a MOI of 50 for 10 hr (viral dose was administered twice, 5 hr apart). The LV used was either clinical-grade 650.MND.hWASp (titer: 2×10^{9} viral particles [Vps]/mL) or non-insulated MND.hWASp (titer: 4.8×10^{8} Vp/mL). After 10-hr viral transduction, donor cells were washed with PBS and 2×10^{6} cells were transferred by intravenous (i.v.) injection into irradiated 6- to 8-week-old *Was*$^{-/-}$ recipients (the irradiation regimen was two 450-cGy doses administered 4 hr apart, the last one immediately prior to transplant). All *Was*$^{-/-}$ recipients had congenically distinct CD45 alleles from that of the donor cells. In parallel, 0.5×10^{6} mock or LV-transduced Lin^{-} BM cells were cultured in vitro in HSC media for 7 days to compare WASp expression and viral copy number of input cells using the two lentiviral constructs.

Assessing Gene Therapy-Treated Mice

The health status of all (primary and secondary) recipient animals post-transplant was evaluated daily by assessment of body condition. Mice that reached predefined humane endpoints were euthanized and analyzed for evidence of clonal expansion of donor or recipient immune cells, histopathology, and serum chemistry. All other recipients were euthanized 16 weeks post-transplant, and tissues were analyzed as described. BM collected from primary recipients at the 16-week time point was also serially transplanted into secondary recipients as described below.

Murine Serum Chemistry and Histological Analyses

PB samples were collected in lithium-coated tubes for CBC and serum chemistry analyses (mouse profile no. 892; Phoenix Central Laboratories) or in heparin for flow cytometry-based immunophenotyping (below). A full necropsy was performed, which included gross visual inspection of all organs and documentation of organomegaly. Major organs were weighed and then fixed in formalin; for the spleen and thymus, sections were removed for formalin fixation, and the remaining spleen and thymus were then re-weighed and processed for immunophenotyping and functional assays described below. Paraffin embedding, sectioning, and hematoxylin and eosin staining were performed by the Histology and Imaging Core at the University of Washington's Department of Comparative Medicine. Organs examined included the heart, skeletal muscle, tongue, thyroid glands, lungs, esophagus, liver, kidneys, adrenal glands, thymus, spleen, salivary glands, stomach, small intestine, cecum, colon, pancreas, reproductive organs, skin, brain (cerebellum and cerebrum), pituitary glands, eyes, harderian glands, ears, and BM.

Murine Immunophenotyping

Thymus and spleen were processed for immunophenotyping and functional assays (below) as follows. Single cell suspensions were obtained by dissociating tissues with frosted glass slides, followed by erythrocytes lysis with ammonium-chloride-potassium buffer (ACK; 0.15 M ammonium chloride, 10.0 mM potassium bicarbonate, and 0.1 mM EDTA) and filtration through a 40-μm mesh. Serum from heparinized PB and BM collected in PBS were also subjected to erythrocyte lysis in ACK and filtration using a 40-μm mesh. Cells were stained with fluorochrome-labeled monoclonal antibodies against cell surface markers, as well as a polyclonal WASp antibody for intracellular WASp expression, using the Cytofix/Cytoperm kit (BD Biosciences) as described.[20] Antibodies used are listed in Table S3. Stained cells were analyzed on an LSR II Flow Cytometer (BD Biosciences) and FACS data were analyzed with FlowJo software (Tree Star). The absolute numbers of splenic and thymic cells were calculated using AccuCount Rainbow Fluorescent beads (SpheroTech), extrapolating from the percentage of each tissue processed. Platelets were isolated from whole peripheral blood and stained for intracellular WASp and platelet surface marker CD41 expression, as described previously.[20]

Murine Secondary Transplantation Experiments

Total BM from each experimental and control gene therapy primary recipient mouse was transplanted into two secondary recipient mice (10×10^{6} cells per mouse). Secondary recipients received the same conditioning regimen as described above and had the same congenic CD45 allele as the primary recipient. Primary recipients with less than 5% WASp expression in myeloid cells, or with less than 20% engraftment of donor myeloid cells, were excluded from secondary BM

transfer experiments. Mice were monitored and analyzed at 16 weeks post-transplantation as described above for the primary recipient mice.

Viral Copy Number Determination

gDNA was extracted from total spleen or BM cells using the QIAmp DNA Blood Mini Kit (QIAGEN). Proviral integrations were detected using the following Gag-specific primers and probe: forward primer (5′-GGAGCTAGAACGATTCGCAGTTA-3′), reverse primer (5′-GGTTGTAGCTGTCCCAGTATTTGTC-3′), and probe (5′-[6FAM]ACAGCCTTCTGATGTTTCTAACAGGCCAGG[BHQ1]-3′). DNA content was normalized using the TaqMan gene expression array for murine β-actin (Life Technologies). Maxima Probe/ROX qPCR Master Mix (Fermentas) was used for amplification with 100 ng input DNA and qPCRs were run on ABI 7500 Real-Time PCR System (Applied Biosystems). Proviral integrations were quantified using a standard curve established using gDNA extracted from a murine B cell line harboring six LV integrations per diploid genome.[61]

Functional Assays of Murine Lymphocytes

Splenic cells were cultured in lymphocyte media (RPMI with 55 μM 2-mercaptoethanol and 10% fetal calf serum), and incubations were at 37°C with 5% CO_2. For testing T cell proliferation, total splenic cells were labeled with CellTrace Violet (Thermo Fisher) and stimulated with 1 μg/mL plate-bound anti-CD3 and 0.25 μg/mL soluble CD28 (clones OKT-3 and 9.3, respectively; University of California, San Francisco Monoclonal Antibody Core), followed by a 72-hr incubation and then flow cytometry for WASp expression and CellTrace Violet dilution. As a positive control, some cells were stimulated with 2 ng/mL PMA and 500 ng/mL ionomycin. The B cell migration assays were performed using CD43-depleted splenocytes (CD43 microbeads; Miltenyi Biotec). One-hundred microliters of cells in lymphocyte media (1×10^6/mL) was seeded in duplicate upper wells of a 5-μm transwell plate (Corning Costar). The lower wells had 600 μL lymphocyte media and 300 nM recombinant murine CXCL13 (R&D Systems). Following a 1-hr incubation, the numbers of cells migrating to the lower well were counted, and the percentage of cells migrating was calculated based on the input cell number.

ELISA

Total serum IgG and IgM levels were quantified by ELISA as described previously.[20] Serum anti-DNA IgG and IgG2c antibodies levels were quantified by ELISA as described.[21]

NHP BM Transplantation

Healthy juvenile pigtailed macaques (*M. nemestrina*) weighing between 3 and 8 kg were housed at the Washington Regional Primate Research Center under conditions approved by AAALAC. All studies and procedures were reviewed and approved by the University of Washington IACUC. Animals were given a 4-day (days −7 to −4) regimen of recombinant human (rh) cytokines including granulocyte colony-stimulating factor (rhG-CSF; 100 μg/kg; Amgen) and stem cell factor (rhSCF; 50 μg/kg; Amgen) as subcutaneous (s.c.) injections. One day later (day −3), marrow volumes totaling ≤10% body weight in kilograms were aspirated from the femora and/or humeri and collected in preservative-free heparin. $CD34^+$ cells were enriched from marrow leukocytes by immunomagnetic column separation. Briefly, cells were incubated with immunoglobulin M monoclonal antibody (clone 12.8) at 4°C for 30 min, washed, and then incubated with rat monoclonal anti-mouse immunoglobulin M microbeads for an additional 30 min at 4°C, followed by immunomagnetic column separation (Miltenyi Biotec) per the manufacturer's instructions. Resulting $CD34^+$ cells were incubated at 37°C and 5% CO_2 in a humidified incubator in StemSpan SFEM media containing 100 ng/mL each of rhSCF, Flt3-L, and thrombopoietin (TPO) for a period of 16–18 hr. Following this pre-stimulation, cells were then divided into equivalent aliquots and were transferred into non-tissue culture-treated vessels pre-coated with 2 μg/cm^2 CH-296 (Retronectin). Cells were exposed to virus at an MOI of 5 infectious units (IU) per cell for 8 hr. An additional volume of virus equivalent to 5 IU/cell was added to each culture and cells were cultured overnight for a final MOI of 10 IU/cell. In preparation for transplantation, animals received myeloablative TBI (1,020 cGy) administered from a linear accelerator at 7 cGy/min in four equally divided fractions over 2 days (days −2 and −1). The following day, cells were harvested and washed and a sample was collected to determine colony-forming capacity and transduction efficiency prior to infusion (day 0) through a central vein catheter. Following transplantation, supportive treatments of rhG-CSF (100 μg/kg) were administered daily i.v. until a neutrophil count of >500/μL was attained for three consecutive counts. Blood product transfusions, antibiotics, and electrolytes were administered as needed.

Analysis of Gene-Modified Cell Engraftment in NHPs

Leukocytes were collected from heparinized PB and BM after ammonium chloride lysis at multiple time points after transplant. Expression of fluorescent proteins (GFP, YFP, mCherry, or BFP) was analyzed by flow cytometry on either a FACS Canto or LSR II cell analyzer (both from BD Biosciences). Fluorochrome expression in lineage-specific populations was determined by gating based on forward and right-angle light scatter characteristics or by expression of lineage-specific CD markers using FlowJo software (version 9 or 10; Tree Star).

Lentivirus Integration Site Analysis in NHP Gene Therapy

gDNA was extracted from leukocytes collected at various time points from either PB or BM or fluorochrome or CD marker-sorted populations by a QIAGEN Blood DNA Mini Kit per the manufacturer's instructions. Lentivirus LTR-genome junctions were amplified by MGS-PCR as described.[48] Resulting sequence libraries were subjected to Ion Torrent semiconductor sequencing and resulting sequence reads were analyzed using the Vector Integration Site Analysis (VISA) server (Grant Trobridge, Washington State University).[62] Genomic sequences were mapped to the rhesus macaque genome (rheMac3) using a stand-alone version of BLAT available from the UCSC Genome Browser (http://genome.ucsc.edu/).[49] Sequences corresponding to the same integration locus were grouped together to determine the total number of unique integration sites (clones)

identified in the sample. Relative contributions of each clone were determined by the number of integration site (IS)-associated sequence reads corresponding to that clone. A quality control check was performed to reveal clones over-represented by PCR bias by comparing the number of IS-associated sequence reads with the number of different fragment lengths observed for each genomic locus.

Statistical Analysis

Statistical analyses were performed with GraphPad Prism version 6 (GraphPad Software). Tests of statistical significance were performed using the unpaired two-tailed Student's t test; p values less than 0.05 were considered significant.

SUPPLEMENTAL INFORMATION

Supplemental Information includes nine figures and three tables and can be found with this article online at http://dx.doi.org/10.1016/j.omtm.2016.11.001.

AUTHOR CONTRIBUTIONS

D.J.R. conceived, designed, and directed the overall project; H.-P.K., J.A., and A.N. designed selected experiments; S.S., I.K., S.K., B.S., M.W., D.L., and Z.N. performed experiments and interpreted results; S.S., K.S., J.A., and D.J.R. wrote the manuscript.

CONFLICTS OF INTEREST

The authors declare that they have no competing financial interests.

ACKNOWLEDGMENTS

Financial support for this work was from the NIH (award numbers R01-AI071163, P01-HL053749, and P01-AI097100), the Fred Hutchinson Cancer Research Center, and the Seattle Children's Hospital Program for Cell and Gene Therapy.

REFERENCES

1. Bosticardo, M., Marangoni, F., Aiuti, A., Villa, A., and Grazia Roncarolo, M. (2009). Recent advances in understanding the pathophysiology of Wiskott-Aldrich syndrome. Blood *113*, 6288–6295.
2. Cavazzana-Calvo, M., Lagresle, C., Hacein-Bey-Abina, S., and Fischer, A. (2005). Gene therapy for severe combined immunodeficiency. Annu. Rev. Med. *56*, 585–602.
3. Notarangelo, L.D., Miao, C.H., and Ochs, H.D. (2008). Wiskott-Aldrich syndrome. Curr. Opin. Hematol. *15*, 30–36.
4. Ochs, H.D., and Thrasher, A.J. (2006). The Wiskott-Aldrich syndrome. J. Allergy Clin. Immunol. *117*, 725–738, quiz 739.
5. Galy, A., and Thrasher, A.J. (2011). Gene therapy for the Wiskott-Aldrich syndrome. Curr. Opin. Allergy Clin. Immunol. *11*, 545–550.
6. Ochs, H.D., and Notarangelo, L.D. (2005). Structure and function of the Wiskott-Aldrich syndrome protein. Curr. Opin. Hematol. *12*, 284–291.
7. Thrasher, A.J., and Burns, S.O. (2010). WASP: a key immunological multitasker. Nat. Rev. Immunol. *10*, 182–192.
8. Marangoni, F., Bosticardo, M., Charrier, S., Draghici, E., Locci, M., Scaramuzza, S., Panaroni, C., Ponzoni, M., Sanvito, F., Doglioni, C., et al. (2009). Evidence for long-term efficacy and safety of gene therapy for Wiskott-Aldrich syndrome in preclinical models. Mol. Ther. *17*, 1073–1082.
9. Ozsahin, H., Cavazzana-Calvo, M., Notarangelo, L.D., Schulz, A., Thrasher, A.J., Mazzolari, E., Slatter, M.A., Le Deist, F., Blanche, S., Veys, P., et al. (2008). Long-term outcome following hematopoietic stem-cell transplantation in Wiskott-Aldrich syndrome: collaborative study of the European Society for Immunodeficiencies and European Group for Blood and Marrow Transplantation. Blood *111*, 439–445.
10. Aiuti, A., Biasco, L., Scaramuzza, S., Ferrua, F., Cicalese, M.P., Baricordi, C., Dionisio, F., Calabria, A., Giannelli, S., Castiello, M.C., et al. (2013). Lentiviral hematopoietic stem cell gene therapy in patients with Wiskott-Aldrich syndrome. Science *341*, 1233151.
11. Boztug, K., Schmidt, M., Schwarzer, A., Banerjee, P.P., Díez, I.A., Dewey, R.A., Böhm, M., Nowrouzi, A., Ball, C.R., Glimm, H., et al. (2010). Stem-cell gene therapy for the Wiskott-Aldrich syndrome. N. Engl. J. Med. *363*, 1918–1927.
12. Hacein-Bey Abina, S., Gaspar, H.B., Blondeau, J., Caccavelli, L., Charrier, S., Buckland, K., Picard, C., Six, E., Himoudi, N., Gilmour, K., et al. (2015). Outcomes following gene therapy in patients with severe Wiskott-Aldrich syndrome. JAMA *313*, 1550–1563.
13. Hacein-Bey-Abina, S., Von Kalle, C., Schmidt, M., McCormack, M.P., Wulffraat, N., Leboulch, P., Lim, A., Osborne, C.S., Pawliuk, R., Morillon, E., et al. (2003). LMO2-associated clonal T cell proliferation in two patients after gene therapy for SCID-X1. Science *302*, 415–419.
14. Howe, S.J., Mansour, M.R., Schwarzwaelder, K., Bartholomae, C., Hubank, M., Kempski, H., Brugman, M.H., Pike-Overzet, K., Chatters, S.J., de Ridder, D., et al. (2008). Insertional mutagenesis combined with acquired somatic mutations causes leukemogenesis following gene therapy of SCID-X1 patients. J. Clin. Invest. *118*, 3143–3150.
15. Braun, C.J., Boztug, K., Paruzynski, A., Witzel, M., Schwarzer, A., Rothe, M., Modlich, U., Beier, R., Göhring, G., Steinemann, D., et al. (2014). Gene therapy for Wiskott-Aldrich syndrome–long-term efficacy and genotoxicity. Sci. Transl. Med. *6*, 227ra33.
16. Mitchell, R.S., Beitzel, B.F., Schroder, A.R., Shinn, P., Chen, H., Berry, C.C., Ecker, J.R., and Bushman, F.D. (2004). Retroviral DNA integration: ASLV, HIV, and MLV show distinct target site preferences. PLoS Biol. *2*, E234.
17. Schröder, A.R., Shinn, P., Chen, H., Berry, C., Ecker, J.R., and Bushman, F. (2002). HIV-1 integration in the human genome favors active genes and local hotspots. Cell *110*, 521–529.
18. Wu, X., Li, Y., Crise, B., and Burgess, S.M. (2003). Transcription start regions in the human genome are favored targets for MLV integration. Science *300*, 1749–1751.
19. Modlich, U., Navarro, S., Zychlinski, D., Maetzig, T., Knoess, S., Brugman, M.H., Schambach, A., Charrier, S., Galy, A., Thrasher, A.J., et al. (2009). Insertional transformation of hematopoietic cells by self-inactivating lentiviral and gammaretroviral vectors. Mol. Ther. *17*, 1919–1928.
20. Astrakhan, A., Sather, B.D., Ryu, B.Y., Khim, S., Singh, S., Humblet-Baron, S., Ochs, H.D., Miao, C.H., and Rawlings, D.J. (2012). Ubiquitous high-level gene expression in hematopoietic lineages provides effective lentiviral gene therapy of murine Wiskott-Aldrich syndrome. Blood *119*, 4395–4407.
21. Becker-Herman, S., Meyer-Bahlburg, A., Schwartz, M.A., Jackson, S.W., Hudkins, K.L., Liu, C., Sather, B.D., Khim, S., Liggitt, D., Song, W., et al. (2011). WASp-deficient B cells play a critical, cell-intrinsic role in triggering autoimmunity. J. Exp. Med. *208*, 2033–2042.
22. Jackson, S.W., Scharping, N.E., Kolhatkar, N.S., Khim, S., Schwartz, M.A., Li, Q.Z., Hudkins, K.L., Alpers, C.E., Liggitt, D., and Rawlings, D.J. (2014). Opposing impact of B cell-intrinsic TLR7 and TLR9 signals on autoantibody repertoire and systemic inflammation. J. Immunol. *192*, 4525–4532.
23. Recher, M., Burns, S.O., de la Fuente, M.A., Volpi, S., Dahlberg, C., Walter, J.E., Moffitt, K., Mathew, D., Honke, N., Lang, P.A., et al. (2012). B cell-intrinsic deficiency of the Wiskott-Aldrich syndrome protein (WASp) causes severe abnormalities of the peripheral B-cell compartment in mice. Blood *119*, 2819–2828.
24. Castiello, M.C., Scaramuzza, S., Pala, F., Ferrua, F., Uva, P., Brigida, I., Sereni, L., van der Burg, M., Ottaviano, G., Albert, M.H., et al. (2015). B-cell reconstitution after lentiviral vector-mediated gene therapy in patients with Wiskott-Aldrich syndrome. J Allergy Clin. Immunol. *136*, 692–702.
25. Pala, F., Morbach, H., Castiello, M.C., Schickel, J.N., Scaramuzza, S., Chamberlain, N., Cassani, B., Glauzy, S., Romberg, N., Candotti, F., et al. (2015). Lentiviral-mediated gene therapy restores B cell tolerance in Wiskott-Aldrich syndrome patients. J. Clin. Invest. *125*, 3941–3951.
26. Challita, P.M., Skelton, D., el-Khoueiry, A., Yu, X.J., Weinberg, K., and Kohn, D.B. (1995). Multiple modifications in cis elements of the long terminal repeat of retroviral

vectors lead to increased expression and decreased DNA methylation in embryonic carcinoma cells. J. Virol. *69*, 748–755.

27. Wielgosz, M.M., Kim, Y.S., Carney, G.G., Zhan, J., Reddivari, M., Coop, T., Heath, R.J., Brown, S.A., and Nienhuis, A.W. (2015). Generation of a lentiviral vector producer cell clone for human Wiskott-Aldrich syndrome gene therapy. Mol. Ther. Methods Clin. Dev. *2*, 14063.

28. Koldej, R.M., Carney, G., Wielgosz, M.M., Zhou, S., Zhan, J., Sorrentino, B.P., and Nienhuis, A.W. (2013). Comparison of insulators and promoters for expression of the Wiskott-Aldrich syndrome protein using lentiviral vectors. Hum. Gene Ther. Clin. Dev. *24*, 77–85.

29. Cartier, N., Hacein-Bey-Abina, S., Von Kalle, C., Bougnères, P., Fischer, A., Cavazzana-Calvo, M., and Aubourg, P. (2010). [Gene therapy of x-linked adrenoleukodystrophy using hematopoietic stem cells and a lentiviral vector]. Bull. Acad Natl. Med. *194*, 255–264, discussion 264–268.

30. Cesana, D., Ranzani, M., Volpin, M., Bartholomae, C., Duros, C., Artus, A., Merella, S., Benedicenti, F., Sergi Sergi, L., Sanvito, F., et al. (2014). Uncovering and dissecting the genotoxicity of self-inactivating lentiviral vectors in vivo. Mol. Ther. *22*, 774–785.

31. Ryu, B.Y., Evans-Galea, M.V., Gray, J.T., Bodine, D.M., Persons, D.A., and Nienhuis, A.W. (2008). An experimental system for the evaluation of retroviral vector design to diminish the risk for proto-oncogene activation. Blood *111*, 1866–1875.

32. Felsenfeld, G., Burgess-Beusse, B., Farrell, C., Gaszner, M., Ghirlando, R., Huang, S., Jin, C., Litt, M., Magdinier, F., Mutskov, V., et al. (2004). Chromatin boundaries and chromatin domains. Cold Spring Harb. Symp. Quant. Biol. *69*, 245–250.

33. Gaszner, M., and Felsenfeld, G. (2006). Insulators: exploiting transcriptional and epigenetic mechanisms. Nat. Rev. Genet. *7*, 703–713.

34. Neff, T., Shotkoski, F., and Stamatoyannopoulos, G. (1997). Stem cell gene therapy, position effects and chromatin insulators. Stem Cells *15* (*Suppl 1*), 265–271.

35. Emery, D.W. (2011). The use of chromatin insulators to improve the expression and safety of integrating gene transfer vectors. Hum. Gene Ther. *22*, 761–774.

36. Raab, J.R., and Kamakaka, R.T. (2010). Insulators and promoters: closer than we think. Nat. Rev. Genet. *11*, 439–446.

37. Arumugam, P.I., Urbinati, F., Velu, C.S., Higashimoto, T., Grimes, H.L., and Malik, P. (2009). The 3′ region of the chicken hypersensitive site-4 insulator has properties similar to its core and is required for full insulator activity. PLoS ONE *4*, e6995.

38. Zhou, S., Fatima, S., Ma, Z., Wang, Y.D., Lu, T., Janke, L.J., Du, Y., and Sorrentino, B.P. (2016). Evaluating the safety of retroviral vectors based on insertional oncogene activation and blocked differentiation in cultured thymocytes. Mol. Ther. *24*, 1090–1099.

39. Astrakhan, A., Ochs, H.D., and Rawlings, D.J. (2009). Wiskott-Aldrich syndrome protein is required for homeostasis and function of invariant NKT cells. J. Immunol. *182*, 7370–7380.

40. Humblet-Baron, S., Sather, B., Anover, S., Becker-Herman, S., Kasprowicz, D.J., Khim, S., Nguyen, T., Hudkins-Loya, K., Alpers, C.E., Ziegler, S.F., et al. (2007). Wiskott-Aldrich syndrome protein is required for regulatory T cell homeostasis. J. Clin. Invest. *117*, 407–418.

41. Snapper, S.B., Rosen, F.S., Mizoguchi, E., Cohen, P., Khan, W., Liu, C.H., Hagemann, T.L., Kwan, S.P., Ferrini, R., Davidson, L., et al. (1998). Wiskott-Aldrich syndrome protein-deficient mice reveal a role for WASP in T but not B cell activation. Immunity *9*, 81–91.

42. Zhang, J., Shehabeldin, A., da Cruz, L.A., Butler, J., Somani, A.K., McGavin, M., Kozieradzki, I., dos Santos, A.O., Nagy, A., Grinstein, S., et al. (1999). Antigen receptor-induced activation and cytoskeletal rearrangement are impaired in Wiskott-Aldrich syndrome protein-deficient lymphocytes. J. Exp. Med. *190*, 1329–1342.

43. Kolhatkar, N.S., Scharping, N.E., Sullivan, J.M., Jacobs, H.M., Schwartz, M.A., Khim, S., Notarangelo, L.D., Thrasher, A.J., Rawlings, D.J., and Jackson, S.W. (2015). B-cell intrinsic TLR7 signals promote depletion of the marginal zone in a murine model of Wiskott-Aldrich syndrome. Eur. J. Immunol. *45*, 2773–2779.

44. Westerberg, L., Larsson, M., Hardy, S.J., Fernández, C., Thrasher, A.J., and Severinson, E. (2005). Wiskott-Aldrich syndrome protein deficiency leads to reduced B-cell adhesion, migration, and homing, and a delayed humoral immune response. Blood *105*, 1144–1152.

45. Modlich, U., Schambach, A., Brugman, M.H., Wicke, D.C., Knoess, S., Li, Z., Maetzig, T., Rudolph, C., Schlegelberger, B., and Baum, C. (2008). Leukemia induction after a single retroviral vector insertion in Evi1 or Prdm16. Leukemia *22*, 1519–1528.

46. Zhou, S., Ma, Z., Lu, T., Janke, L., Gray, J.T., and Sorrentino, B.P. (2013). Mouse transplant models for evaluating the oncogenic risk of a self-inactivating XSCID lentiviral vector. PLoS ONE *8*, e62333.

47. Kiem, H.P., Arumugam, P.I., Burtner, C.R., Fox, C.F., Beard, B.C., Dexheimer, P., Adair, J.E., and Malik, P. (2014). Pigtailed macaques as a model to study long-term safety of lentivirus vector-mediated gene therapy for hemoglobinopathies. Mol. Ther. Methods Clin. Dev. *1*, 14055.

48. Beard, B.C., Adair, J.E., Trobridge, G.D., and Kiem, H.P. (2014). High-throughput genomic mapping of vector integration sites in gene therapy studies. Methods Mol. Biol. *1185*, 321–344.

49. Rosenbloom, K.R., Armstrong, J., Barber, G.P., Casper, J., Clawson, H., Diekhans, M., Dreszer, T.R., Fujita, P.A., Guruvadoo, L., Haeussler, M., et al. (2015). The UCSC Genome Browser database: 2015 update. Nucleic Acids Res. *43*, D670–D681.

50. Forbes, S.A., Beare, D., Gunasekaran, P., Leung, K., Bindal, N., Boutselakis, H., Ding, M., Bamford, S., Cole, C., Ward, S., et al. (2015). COSMIC: exploring the world's knowledge of somatic mutations in human cancer. Nucleic Acids Res. *43*, D805–D811.

51. Lacout, C., Haddad, E., Sabri, S., Svinarchouk, F., Garçon, L., Capron, C., Foudi, A., Mzali, R., Snapper, S.B., Louache, F., et al. (2003). A defect in hematopoietic stem cell migration explains the nonrandom X-chromosome inactivation in carriers of Wiskott-Aldrich syndrome. Blood *102*, 1282–1289.

52. Shepherd, B.E., Kiem, H.P., Lansdorp, P.M., Dunbar, C.E., Aubert, G., LaRochelle, A., Seggewiss, R., Guttorp, P., and Abkowitz, J.L. (2007). Hematopoietic stem-cell behavior in nonhuman primates. Blood *110*, 1806–1813.

53. Trobridge, G.D., and Kiem, H.P. (2010). Large animal models of hematopoietic stem cell gene therapy. Gene Ther. *17*, 939–948.

54. Kiem, H.P., Baum, C., Bushman, F.D., Byrne, B.J., Carter, B.J., Cavagnaro, J., Malech, H.L., Mendell, J.R., Naldini, L.M., Sorrentino, B.P., et al. (2014). Charting a clear path: the ASGCT Standardized Pathways Conference. Mol. Ther. *22*, 1235–1238.

55. Hanawa, H., Hematti, P., Keyvanfar, K., Metzger, M.E., Krouse, A., Donahue, R.E., Kepes, S., Gray, J., Dunbar, C.E., Persons, D.A., and Nienhuis, A.W. (2004). Efficient gene transfer into rhesus repopulating hematopoietic stem cells using a simian immunodeficiency virus-based lentiviral vector system. Blood *103*, 4062–4069.

56. Hanawa, H., Yamamoto, M., Zhao, H., Shimada, T., and Persons, D.A. (2009). Optimized lentiviral vector design improves titer and transgene expression of vectors containing the chicken beta-globin locus HS4 insulator element. Mol. Ther. *17*, 667–674.

57. Petrella, A., Doti, I., Agosti, V., Giarrusso, P.C., Vitale, D., Bond, H.M., Cuomo, C., Tassone, P., Franco, B., Ballabio, A., et al. (1998). A 5′ regulatory sequence containing two Ets motifs controls the expression of the Wiskott-Aldrich syndrome protein (WASP) gene in human hematopoietic cells. Blood *91*, 4554–4560.

58. Hanawa, H., Kelly, P.F., Nathwani, A.C., Persons, D.A., Vandergriff, J.A., Hargrove, P., Vanin, E.F., and Nienhuis, A.W. (2002). Comparison of various envelope proteins for their ability to pseudotype lentiviral vectors and transduce primitive hematopoietic cells from human blood. Mol. Ther. *5*, 242–251.

59. Hanawa, H., Persons, D.A., and Nienhuis, A.W. (2005). Mobilization and mechanism of transcription of integrated self-inactivating lentiviral vectors. J. Virol. *79*, 8410–8421.

60. Kerns, H.M., Ryu, B.Y., Stirling, B.V., Sather, B.D., Astrakhan, A., Humblet-Baron, S., Liggitt, D., and Rawlings, D.J. (2010). B cell-specific lentiviral gene therapy leads to sustained B-cell functional recovery in a murine model of X-linked agammaglobulinemia. Blood *115*, 2146–2155.

61. Sather, B.D., Ryu, B.Y., Stirling, B.V., Garibov, M., Kerns, H.M., Humblet-Baron, S., Astrakhan, A., and Rawlings, D.J. (2011). Development of B-lineage predominant lentiviral vectors for use in genetic therapies for B cell disorders. Mol. Ther. *19*, 515–525.

62. Hocum, J.D., Battrell, L.R., Maynard, R., Adair, J.E., Beard, B.C., Rawlings, D.J., Kiem, H.P., Miller, D.G., and Trobridge, G.D. (2015). VISA–Vector Integration Site Analysis server: a web-based server to rapidly identify retroviral integration sites from next-generation sequencing. BMC Bioinformatics *16*, 212.

OMTM, Volume *4*

Supplemental Information

Safe and Effective Gene Therapy for Murine Wiskott-Aldrich Syndrome Using an Insulated Lentiviral Vector

Swati Singh, Iram Khan, Socheath Khim, Brenda Seymour, Karen Sommer, Matthew Wielgosz, Zachary Norgaard, Hans-Peter Kiem, Jennifer Adair, Denny Liggitt, Arthur Nienhuis, and David J. Rawlings

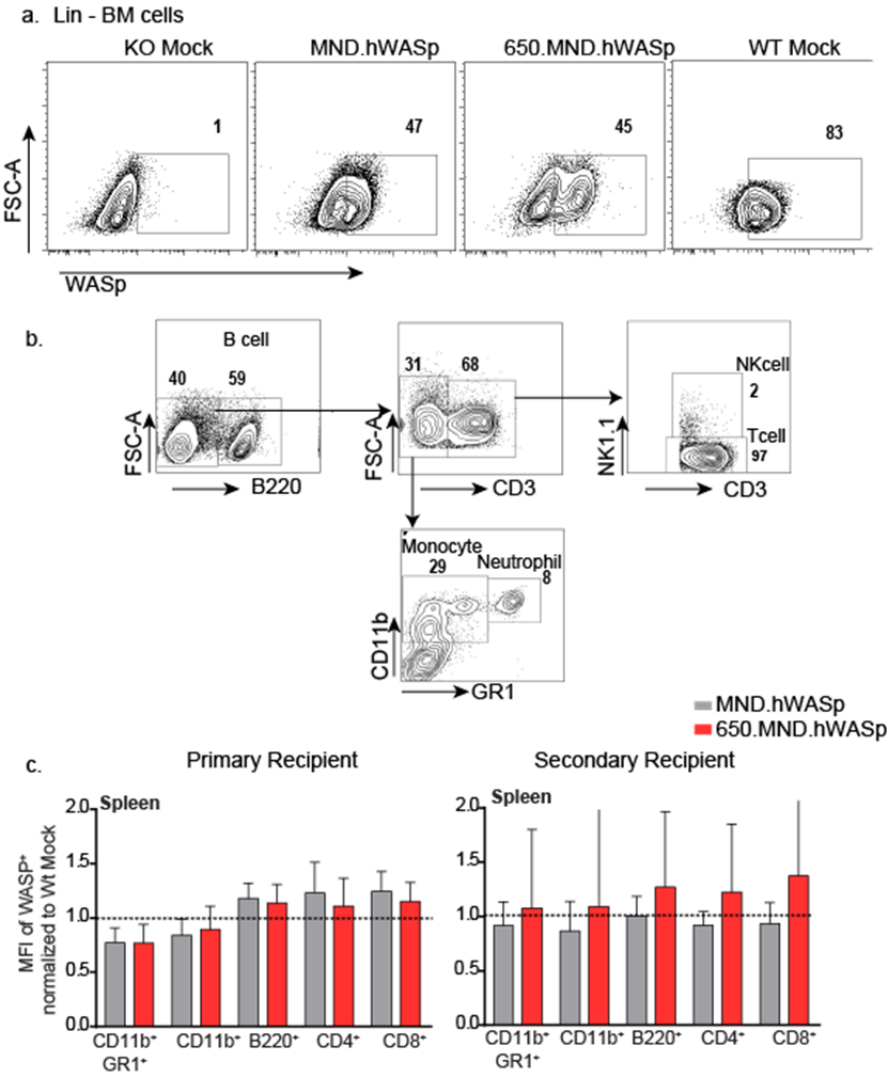

Figure S1. LV-delivered WASp expression is similar to that of endogenous *WAS* across multiple hematopoietic lineages. (**a)** Representative FACS plots of WASp expression after *in vitro* transduction of *Was*$^{-/-}$ mouse lin^{-} BM cells with either MND.hWASp or 650.MND.hWASp LV, or mock transduced *Was*$^{-/-}$ (KO) or WT lin^{-} BM cells. After transduction, cells were cultured for 7 days in StemSpan media supplemented with murine SCF and TPO cytokines. The percentage of WASp^{+} live cells is indicated. (**b)** Flow cytometry gating strategy for determining hematopoietic subsets. The same antibody panel was used for peripheral blood, BM and spleen. (**c)** Mean fluorescence intensity (MFI) of WASp^{+} cells in splenic hematopoietic cell subsets of primary and secondary recipients normalized to WT mock, shown as mean ± SD. For primary recipients, n = 3 (WT Mock), 5 (MND.hWASp), and 12 (650.MND.hWASp); for secondary recipients, n = 15 (WT Mock), 16 (MND.hWASp), and 50 (650.MND.hWASp).

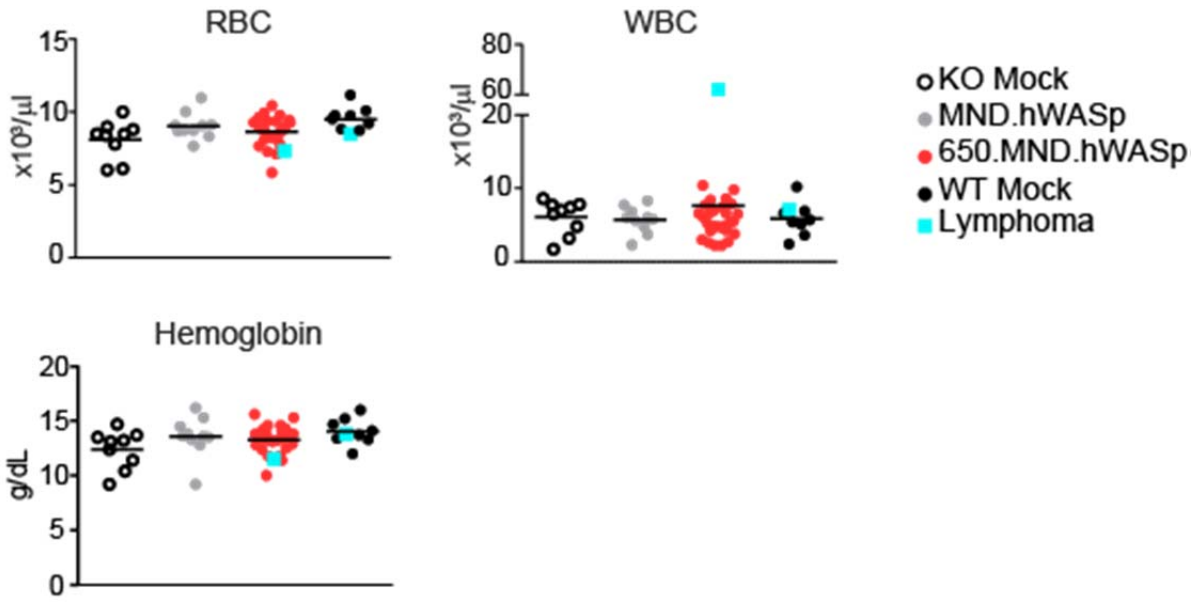

Figure S2. Peripheral blood cell counts for primary LV and control gene therapy recipients. Values from peripheral blood obtained 16 weeks post-transplant. Results are from 3 individual experiments; n =10 (KO Mock and MND.hWASp), 9 (WT Mock) and 29 (650.MND.hWASp). Mice with lymphomas are indicated in blue within their gene therapy cohort. RBC = Red blood cell; WBC = white blood cell.

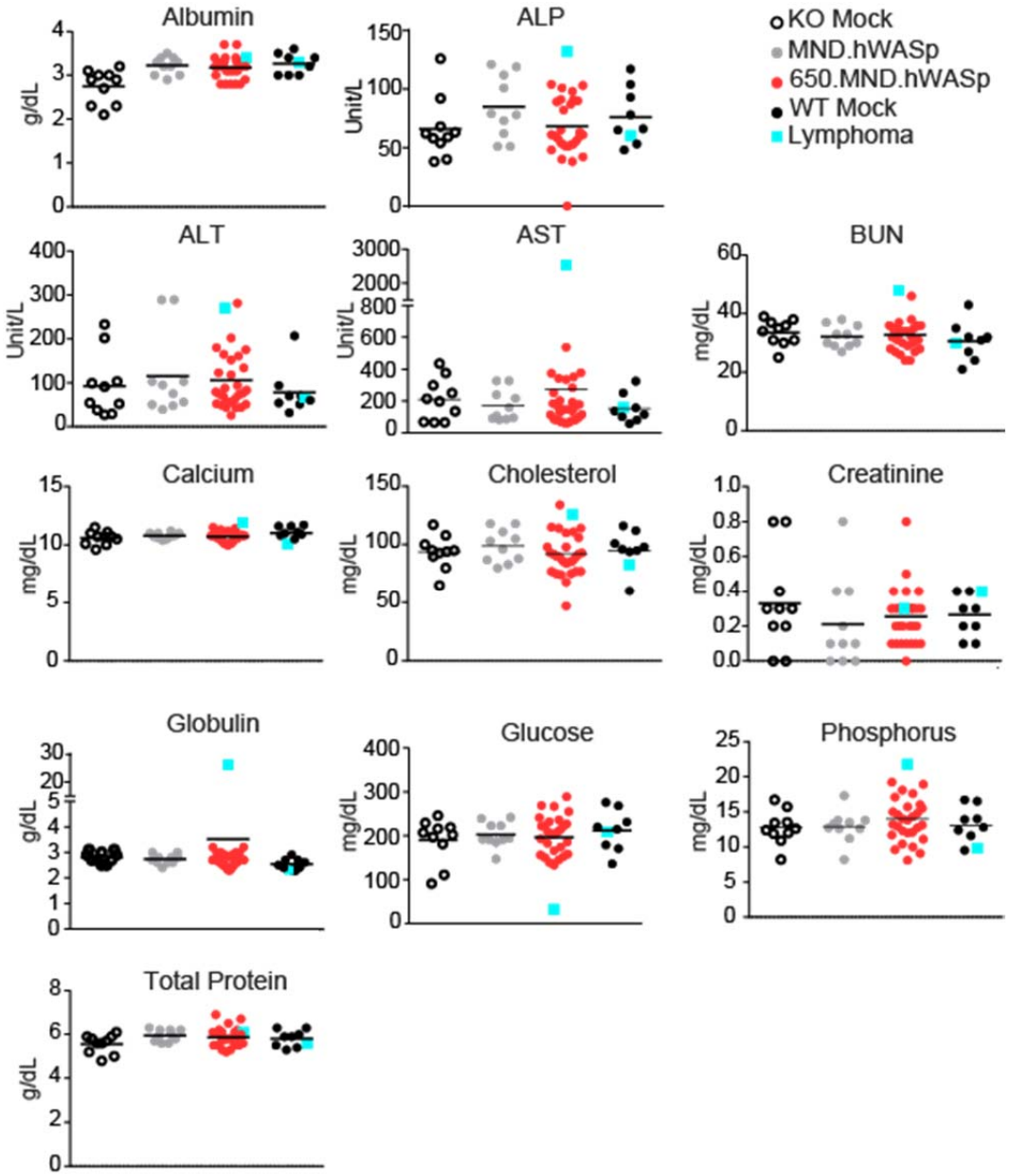

Figure S3: Serum chemistry for primary LV and control gene therapy recipients. Values from peripheral blood obtained 16 weeks post-transplant. Results compiled from 3 individual experiments; n =10 (KO Mock and MND.hWASp), 9 (WT Mock) and 29 (650.MND.hWASp). Mice with lymphomas are indicated in blue within their gene therapy cohort. ALP = alkaline phosphatase; ALT = alanine aminotransferase; AST = aspartate aminotransferase; BUN = blood urea nitrogen.

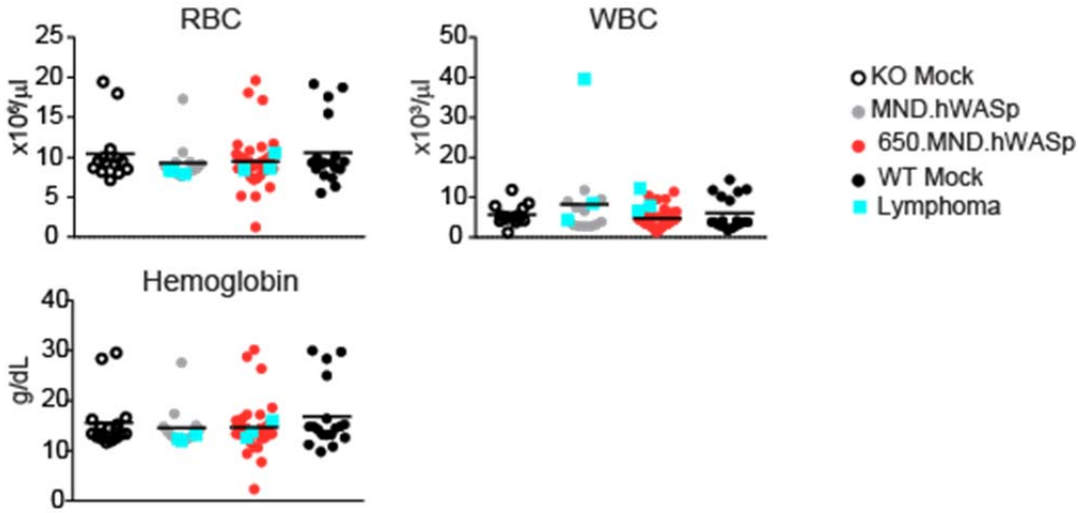

Figure S4. Peripheral blood cell counts for secondary LV and control gene therapy recipients. Values from peripheral blood obtained 16 weeks post-transplant. Results compiled from 3 individual experiments; n = 14 (KO and MND.hWASp), 18 (WT Mock) and 52 (650.MND.hWASp). Mice with lymphomas are indicated in blue within their gene therapy cohort. RBC = Red blood cell; WBC = white blood cell.

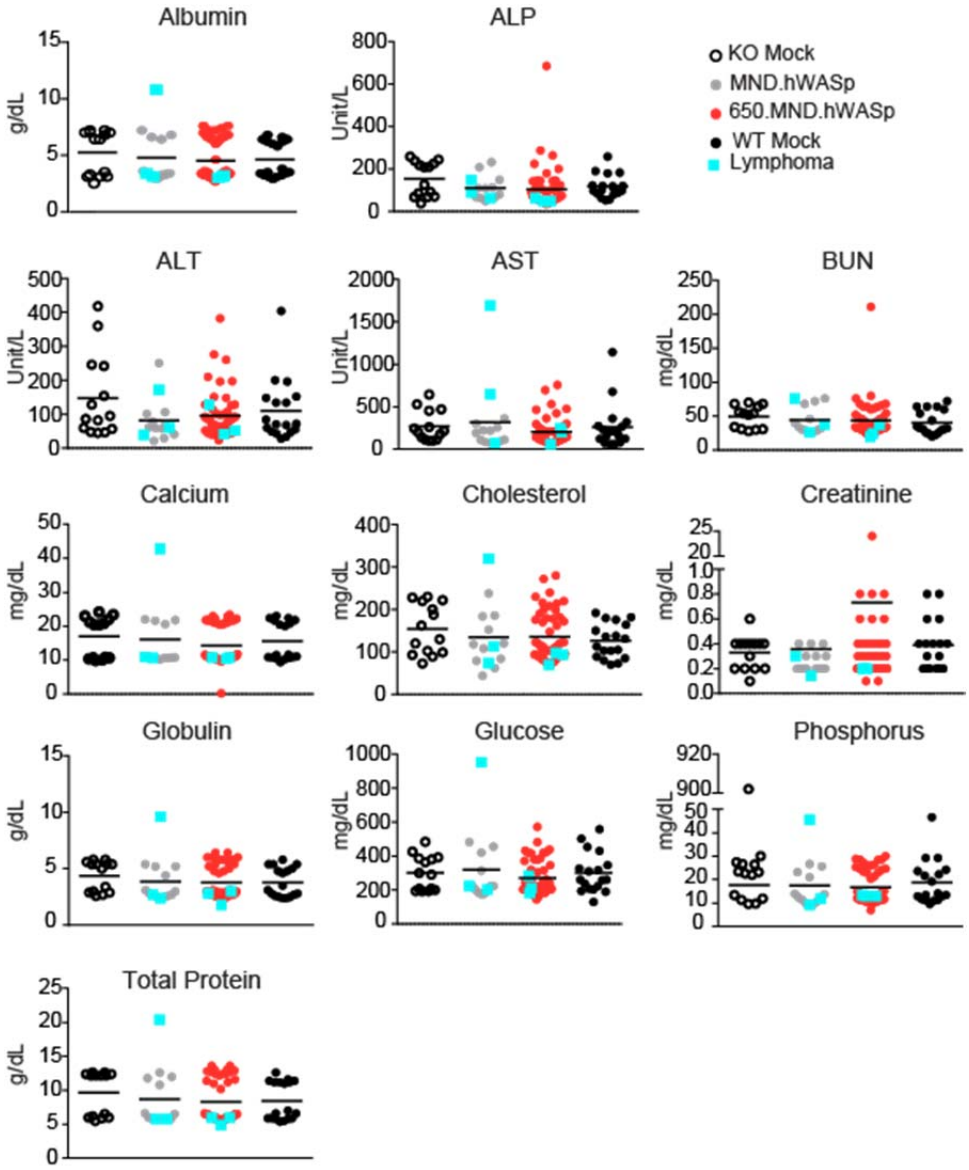

Figure S5. Serum chemistry for secondary LV and control gene therapy recipients. Values from peripheral blood obtained 16 weeks post-transplant. Results compiled from 3 individual experiments; n = 14 (KO and MND.hWASp), 18 (WT Mock) and 52 (650.MND.hWASp). Mice with lymphomas are indicated in blue within their gene therapy cohort. ALP = alkaline phosphatase; ALT = alanine aminotransferase; AST = aspartate aminotransferase; BUN = blood urea nitrogen.

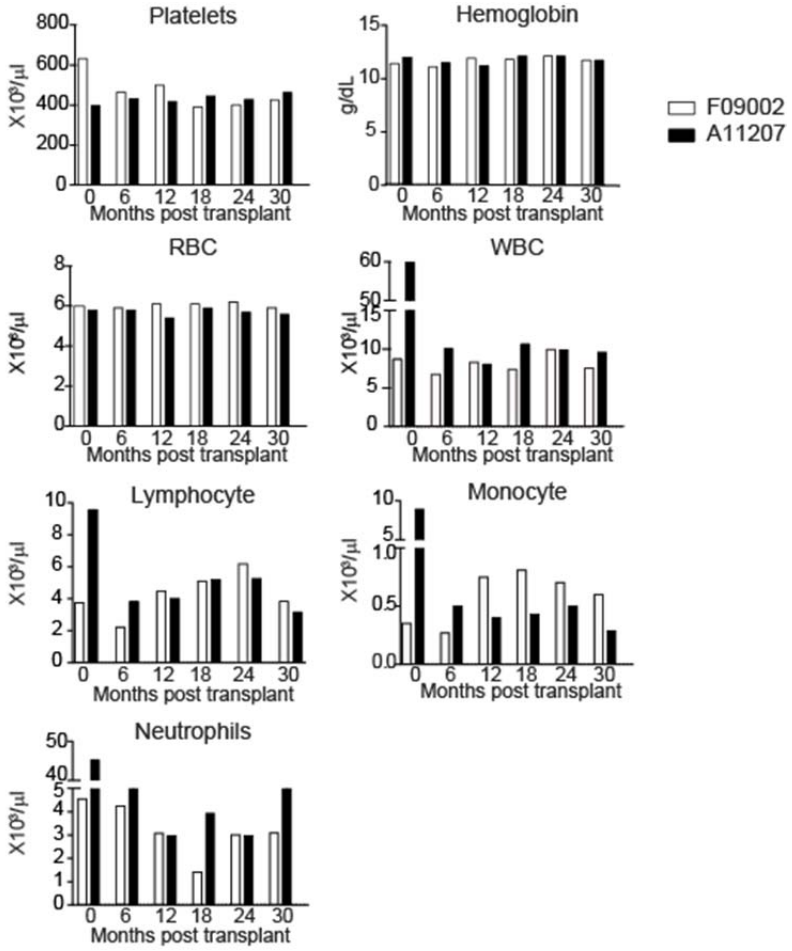

Figure S6. Peripheral blood cell counts for non-human primates F09002 and A11207. Time course of cell counts on the indicated month post-transplant with gene therapy treated cells. RBC = Red blood cell; WBC = white blood cell.

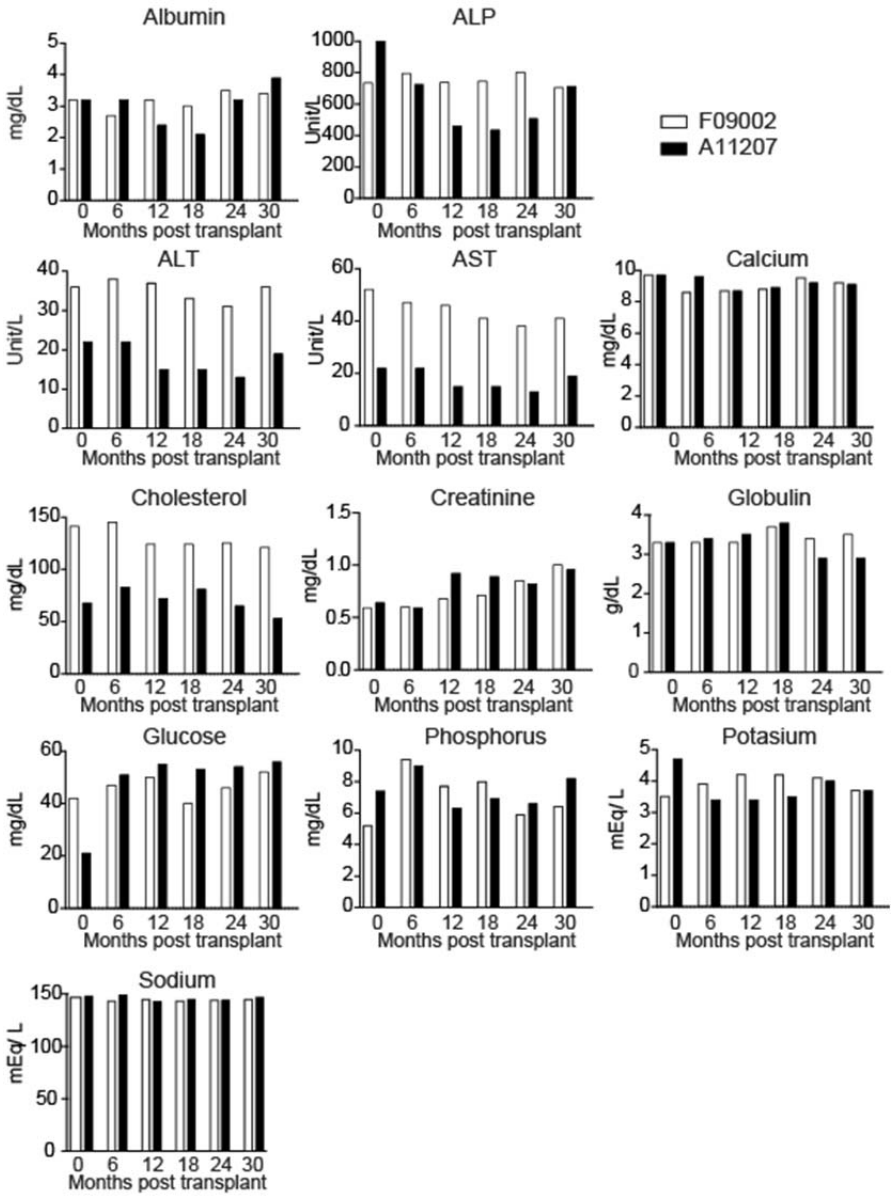

Figure S7. Serum chemistry for non-human primates F09002 and A11207. Time course of serum chemistry on the indicated month post-transplant with gene therapy treated cells. ALP = alkaline phosphatase; ALT = alanine aminotransferase; AST = aspartate aminotransferase; BUN = blood urea nitrogen.

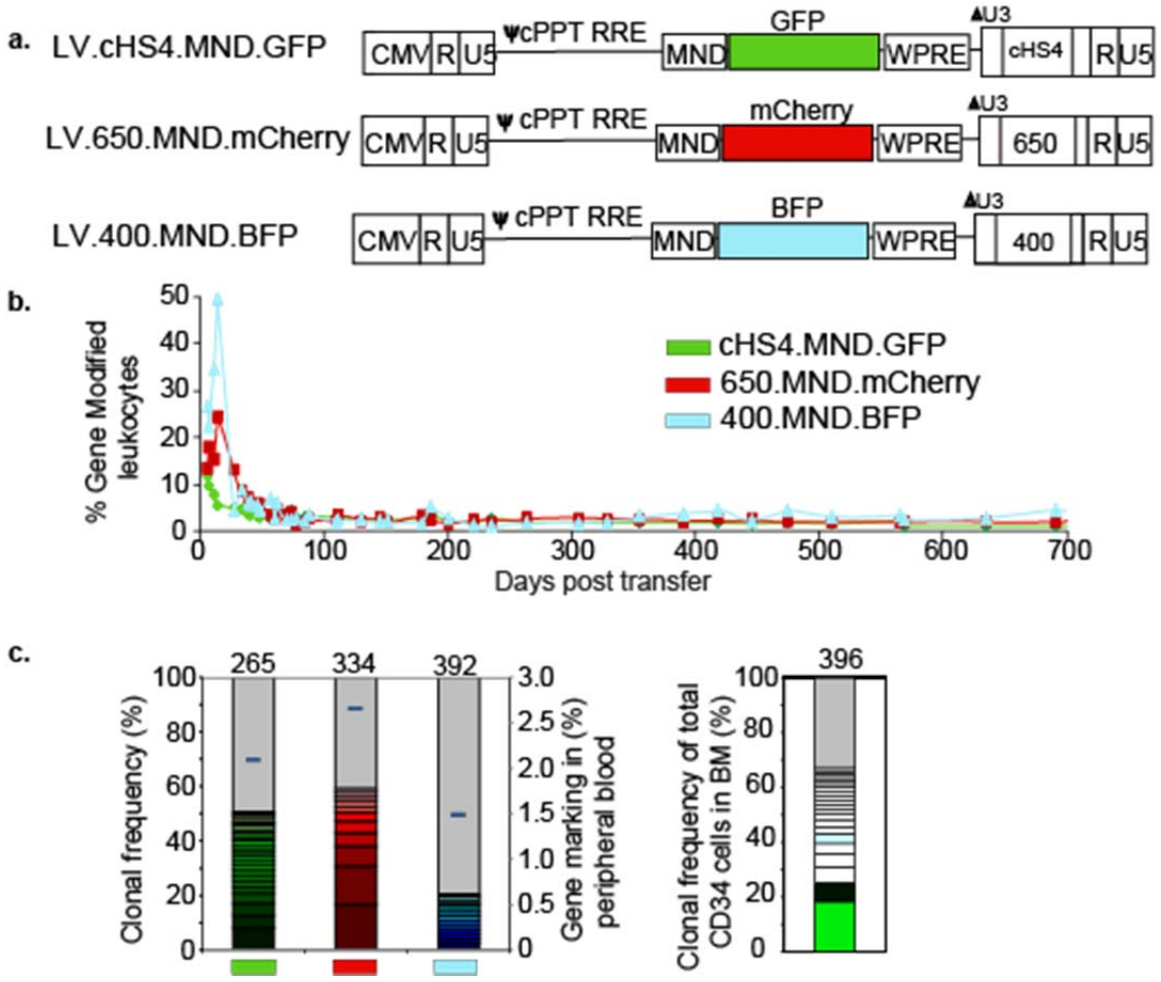

Figure S8. Direct comparison of expression and polyconality of insulated and non-insulated MND promoters in a non-human primate gene therapy model. (a) Schematic diagram of the SIN-LV vectors used for this study. All LV vectors were based on the SIN LV pCL backbone. *Macaca nemestrina* #A11207 was transplanted with bone marrow transduced with three different SIN-LV MND-fluorochrome expression cassettes, each insulated using a distinct fragment of the 1.2 kb cHS4 chromatin insulating element. The GFP expression cassette was insulated by the full-length insulator, mCherry was insulated by the 650 bp cHS4 fragments, and BFP was insulated by a 400 bp fragment as described (Arumugon et at, Wielgosz et al). **(b)** Plot shows % lentivirus transduced leukocytes in peripheral blood vs. time post-transfer. Fluorophores are from the LV in (**a**) and were detected using flow cytometry. **(c)** Clonal diversity of sorted fluorochrome^{+} peripheral blood (*left*) and BM CD34^{+} (*right*) leukocytes in animal A11207 221 days (peripheral blood) or 223 days (BM CD34+ cells) after transplant**.** The thickness of the colored bars indicates the frequency of a particular clone; clones in the gray shaded area are too infrequent to distinguish width. The total number of clones identified in each sample is listed at the top of the corresponding bar. The percentage of fluorochrome^{+} cells within peripheral blood (*right y-axis*) is indicated by a dark blue bar.

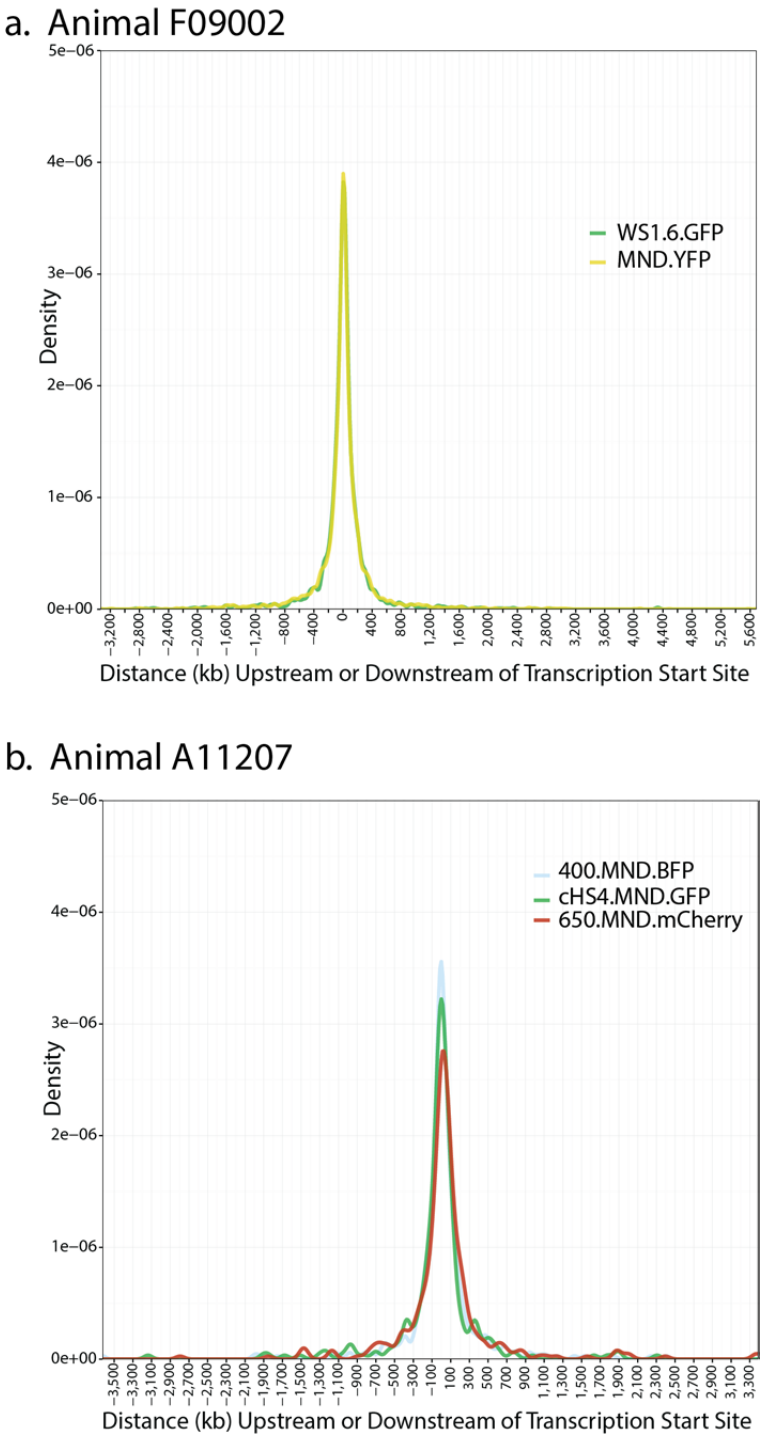

Figure S9. Integration Site Distances to Transcription Start Sites. Integration Site Distances to Transcription Start Sites. The probability density function was calculated using a Kernel Density Estimation (*geom_density* function of the *ggplot2 R* package) of distance between integration site and transcription start site for each fluorescent protein (colored) in subject (**a**) F09002 and (**b**) A11207. The area under the curve sums to 1. The probability of observing an integration site in any given window is given as the area under the curve between those two points on the x axis. Upstream and downstream are relative to the direction of transcription.

Group	Experimentally Induced Background Lesions	Primary Mice Total/Affected	Secondary Mice Total/Affected
650 MND hWAS-M	Rad-Pneumonitis	20/19	44/37
	Rad-Glomerulopathy	20/20	44/44
	Rad-Testicular Atrophy	20/19	44/44
	Collection trauma	20/18	44/40
650 MND hWAS-F	Rad-Pneumonitis	10/9	9/8
	Rad-Glomerulopathy	10/9	9/8
	Rad-Ovarian Atrophy	10/10	9/8
	Collection trauma	10/9	9/7
KO Mock-M	Rad-Pneumonitis	7/7	3/3
	Rad-Glomerulopathy	7/7	3/3
	Rad-Testicular Atrophy	7/7	3/3
	Collection trauma	7/7	3/3
KO Mock-F	Rad-Pneumonitis	3/2	11/8
	Rad-Glomerulopathy	3/3	11/11
	Rad-Ovarian Atrophy	3/1	11/11
	Collection trauma	3/3	11/10
WT Mock-M	Rad-Pneumonitis	5/4	6/6
	Rad-Glomerulopathy	5/5	6/6
	Rad-Testicular Atrophy	5/5	6/6
	Collection trauma	5/4	6/6
WT Mock-F	Rad-Pneumonitis	4/3	9/9
	Rad-Glomerulopathy	4/3	9/9
	Rad-Ovarian Atrophy	4/4	9/9
	Collection trauma	4/2	9/7

Table S1. Background histopathology lesions identified in the murine gene therapy controls. Rad = lesions found in all cohorts receiving total body irradiation.

Days Post Transplant	Chromosome	Locus of Integration (bp)	Nearest Oncogene TSS (kb)	Nearest TSS Oncogene Name	IS Genomic Feature
96	5	146057509-146057541	69.4	FBXW7	Intronic (FBXW7)
	11	62386621-62386439	33.0	WIF1	Intronic (WIF1)
221	1	60908469-60908512	1210.8	JUN	Intergenic
	4	37524395-37524458	142.1	HMGA1	Intergenic
	7	144707316-144707370	124.2	GTF2A1	Intronic (TSHR)
	8	95057086-95057034	128.0	NBN	Intergenic
	11	63162615-63162678	38.0	HMGA2	Intronic (HMGA2)
	12	60750713-60750671	68.4	SF3B1	Intergenic
	13	132794273-132794169	110.7	ERCC3	Intergenic
	13	47318184-47318119	171.7	FBXO11	Intergenic
	13	61658259-61658311	51.5	XPO1	Intergenic
	15	89202976-89203017	1652.1	GNAQ	Intergenic
	20	4182934-4182988	202.3	CREBBP	Intergenic
	X	154605195-154605319	29.8	MTCP1NB	Intronic (MTCP1)
392	5	146057509-146057541	69.4	FBXW7	Intronic (FBXW7)
	7	129555065-129554970	25.7	GPHN	Intronic (GPHN)
	11	48069006-48069149	3.4	ATF1	Intronic (ATF1)
	14	114860698-114860772	194.0	ZBTB16	Intergenic
	16	32431104-32431030	99.4	CDK12	Intergenic
	16	62004778-62004811	58.0	DDX5	Intergenic
	20	65374479-65374403	62.8	CBFB	Intronic (CBFB)

Table S2. Lentivirus insertion sites associated with known oncogenes for animal A11207. Genes proximal to the integration sites identified at different time points (96, 221 and 392 days after transplant) are shown. Yellow highlight shows clones with identical integration sites. TSS= Transcription start site, IS= integration site.

Mouse antigen:	Fluorophore	Clone	Supplier
B220	QDot 655	RA3-6B2	Life Technologies
CD11b	FITC	M1/70	eBioscience
GR-1	eFluor450	RB6-8C5	eBioscience
NK1.1	PE	PK163	Biolegend
CD3	APC-Cy7	17A2	eBioscience
CD45.2	Pe-Cy7	104	Southern BioTech
CD45.1	APC	A20	eBioscience
CD62L	APC	MEL-14	eBioscience
CD25	FITC	PC61	Biolegend
CD44	APC-Cy7	IM7	Biolegend
CD8	PE	53- 6.7	eBioscience
CD4	PerCp-Cy5.5	GK1.5	Biolegend
CD45.1	Pacific Blue	A20	eBioscience
CD23	APC	B3B4	Life Technologies
CD21	PE	7G6	BD Bioscience
CD45.1	FITC	A20	eBioscience
CD24	Pacific Blue	M1/69	Biolegend
Sca-1	PerCp-Cy5.5	D7	eBioscience
c-Kit	PE	2B8	eBioscience
CD41	FITC	MWReg30	BD Bioscience
Mouse hematopoietic lineage cocktail	eFluor450	17A2, RA3-6B2, M1/70, TER-119, RB6-8C5	eBioscience
WASp			Hans Ochs
F(ab\')2 anti-rabbit IgG	Alexa568	polyclonal	Life Technologies

Table S3. List of antibodies used for flow cytometry.